iScience

CellPress
OPEN ACCESS

Review

Insights into the hydrogen generation and catalytic mechanism on Co-based nanocomposites derived from pyrolysis of organic metal precursor

Huanhuan Zhang,[1,2] Shuling Liu,[2] Yanyan Liu,[2,3,*] Tongjun Li,[2] Ruofan Shen,[2] Xianji Guo,[2] Xianli Wu,[2] Yushan Liu,[2] Yongfeng Wang,[4] Baozhong Liu,[5] Erjun Liang,[2] and Baojun Li[2,6,*]

SUMMARY

Hydrogen generation from boron hydride is important for the development of hydrogen economy. Cobalt (Co) element has been widely used in the hydrolysis of boron hydride. Pyrolysis is a common method for materials synthesis in catalytic fields. Herein, Co-based nanocomposites derived from the pyrolysis of organic metal precursors and used for hydrolysis of boron hydride are summarized and discussed. The different precursors consisting of MOF, supported, metal, and metal phosphide precursors are summarized. The catalytic mechanism consisting of dissociation mechanism based on oxidative addition-reduction elimination, pre-activation mechanism, SN2 mechanism, four-membered ring mechanism, and acid-base mechanism is intensively discussed. Finally, conclusions and outlooks are conveyed from the design of high-efficiency catalysts, the characterization of catalyst structure, the enhancement of catalytic activities, the investigation of the catalytic mechanism, and the catalytic stability of active structure. This review can provide guidance for designing high-efficiency catalysts and boosting development of hydrogen economy.

INTRODUCTION

The significance of hydrogen generation

With social development and the improvement in human lifestyle, the energy demand continuously increases and energy is regarded as the most important problem facing humanity. Hydrogen, as an attractive energy carrier and environmentally friendly fuel, is promising in the development of an energy economy because of its high energy density, sustainability, and socioeconomic/environmental advantages.[1–4] Hydrogen is the lightest of all the elements with a density of 0.0899 g/L in standard state and the value is one ten-thousandth the density of water. Additionally, at −252.7°C, it can be liquid following a density of 70 g/L, and this value is only 1/15th of water. Thus, there remains a considerable challenge to create highly efficient technology for the storage of hydrogen. Conventional methods such as physical storage, the acceptable gravimetric and volumetric storage capacities only can be obtained at up to 800 bar high pressure or cryogenic temperature (−253°C). Such conditions require sophisticated technologies and pose safety problems.[5] Recently, the development of sustainable technologies, such as solar water splitting[6–8] and clean-zero carbon emission[9–11] and so on are important for the hydrogen economy. Illustratively, the chemical hydride storage and release of hydrogen is a promising way of development in the field of hydrogen generation. The reasons are as follows: (1) The presence of a large amount of water increases stability by preventing combustion; (2) kinetically stable, it does not release hydrogen without appropriate catalysts; and (3) hydrogen generation is controllable according to practical needs. Thus, the catalytic hydrolytic dehydrogenation of chemical hydrides is a safe and efficient way to provide hydrogen fuel for new energy vehicles and portable electronic devices. Currently, cost-efficient and high-performance catalysts must be developed before the large-scale application of this hydrogen generation technology can proceed. Chemical hydrides, such as SB, AB, and $N_2H_4BH_3$ with high densities of available hydrogen, are considered convenient hydrogen sources through hydrolysis or pyrolysis. The development of earth-abundant catalysts for efficient hydrolysis of boron hydride is of great importance in the conversion and utilization of hydrogen energy. Despite great progresses being made in recent years, all the reported heterogeneous catalysts up to now involve noble metals greatly limits their large-scale practical application because of their high cost and insufficient reserves in the Earth's crust. Therefore, the development of a cost-effective noble-metal-free

[1]School of Chemistry and Chemical Engineering, Henan University of Technology, 100 Lianhua Road, Zhengzhou 450001, P.R.China
[2]College of Chemistry, Zhengzhou University, 100 Science Road, Zhengzhou 450001, P.R.China
[3]College of Science, Henan Agriculture University, 63 Nongye Road, Zhengzhou 450002, P.R.China
[4]Center for Carbon-based Electronics and Key Laboratory for the Physics and Chemistry of Nanodevices, Department of Electronics, Peking University, Beijing 100871, P.R.China
[5]College of Chemistry and Chemical Engineering, Henan Polytechnic University, 2001 Century Avenue, Jiaozuo 454000, P.R.China
[6]Department of Chemistry, Tsinghua University, Beijing 100084, P.R.China
*Correspondence: lyylhs180208@163.com (Y.L.), lbjfcl@zzu.edu.cn (B.L.)
https://doi.org/10.1016/j.isci.2024.109715

catalyst is imperative for hydrogen generation by boron hydride, possibly Fe, Ni, Cu, or Co. Cobalt is an efficient metal catalyst and has already proven to be a potential alternative to noble metals. Recently, Co-based catalysts have caused concern for hydrogen generation of boron hydride. The non-noble metal Co has the advantage of abundant coordination forms and adjustable redox ability. The existence of Co is found in a mixed valence state under AB reaction conditions and can provide a structural basis for the formation of multi-active sites. Illustratively, the elements Fe, Ni, and Cu present a single/stable valence state during the reaction of AB hydrolysis, thus, Co-based catalysts exhibit superiority compared to Fe, Ni, Cu, and their derived catalysts.[12] However, the strong reducibility of the low-valent B and active H species produced during the reaction will decrease the catalytic activity of the Co-based catalyst. The Co nanoparticles NPs with the ferromagnetism would force the catalyst to be driven by its magnetism, which called self-stirring mode during the hydrolysis of AB. The self-stirring mode means that the reaction system was stirred by an external magnetic field through the ferromagnetic catalysts in the absence of magneton. Due to the existence of magnetism, magnetons are not necessary and this is wonderful for cyclic hydrogen generation, namely, the reaction products from the reactant circumstances can be smoothly separated and start the next activity testing of hydrogen generation. Additionally, from the literature, the catalytic activity of cobalt and cobalt oxides is significantly increased supported by related experimental results.[13–15] When the catalyst is prepared through support on the foam nickel, carbon cloth, or other substrates, the obtained catalysts can be stopped at any time in catalytic hydrogen generation, which has more value for future industrial application. Additionally, on-demand hydrogen generation from the hydrolysis reactions of chemical hydrides has gained ever-increasing attention as a promising approach for providing mobile/portable hydrogen sources. Therefore, the design and synthesis of effective catalysts for releasing hydrogen is the decisive factor.

The importance of catalysts design

The design of heterogeneous catalysts relies on an understanding of the fundamental surface dynamics that govern the performance of catalysts. The rational design of the catalysts can expose more active sites and play an important role in the enhancement of the catalytic performance.[16,17] The reaction of boron hydride hydrolysis involves a bimolecular reaction and the active ingredient in designed catalyst should has the ability to activate boron hydride and water molecules. Based on the catalytic activity and catalytic mechanism, the rational design of the catalysts has a significant role in conveying the design idea. The purpose of catalyst design is to select the most efficient catalyst for a reaction using established concepts and simultaneously determine the preparation method and use conditions of the catalyst. The main contents of the catalyst design include the reaction target, source of raw materials, comprehensive consideration of economic rationality, thermodynamic analysis, the design of the reaction process, the selection of active components, additives, supports types in the catalysts, the kinetic test inspection and determination of operating conditions and so on. The design strategy is suitable for the high-efficiency catalysts and many methods have been used in the preparation of precursors, such as deposition-precipitation method,[18] one-step hydrothermal method,[19,20] sol-gel method,[21] leaching method,[22] ion exchange method,[23] thermal melting,[24] and so on. The different methods have different advantages and disadvantages for the preparation of catalysts. The deposition-precipitation method can ensure all the active components are retained on the surface of the support, which improves the utilization rate of active components. However, some problems exist in this method: (1) The control of the sediment location; (2) the nucleation process is more likely to occur in solution than on a support; and (3) the generated metal particles have low uniformity. Although the one-step hydrothermal method is simple, short in process, and low in synthesis cost, it is not applicable for the synthesis of water-sensitive compounds, such as III–V semiconductors, novel phosphorus (or arsenic), or acid molecular sieve skeleton structure materials. The sol-gel method occurs under low temperature conditions and can produce small/uniform particle size. The sol-gel method incurs high cost because of the use of metal alkoxides as raw materials. The leaching method is simple, efficient, fast, and with a wide range of applications; however, it is difficult to control the leaching time and leaching agent concentration. The ion exchange method has the advantage of removing inorganic ions, but the exchange capacity is limited. From the above-mentioned methods, the different strategies have different effects on the construction of active structures and will lead to different influences on the performance of different reactions. Among the many metal-based preparation methods, metal ion pyrolysis is the most common method in synthesizing the corresponding materials. Pyrolysis has become a common method in materials synthesis in many aspects of catalytic fields because of the low demand for experimental equipment in metal ion pyrolysis. Therefore, the usage of pyrolysis technology to design catalysts or the catalyst structure is vital for the profound research in the field of heterogeneous catalysis. Based on the operation of pyrolysis, the discussion of scientific problems of catalyst design will have excellent significance on the enhancement of catalytic activity and the confirmation of the structure-activity relationship.

The scope of the review

Currently, the investigation of Co-based materials derived from pyrolysis of organic metal precursors has drawn enormous attention and applied many physical and chemical fields. The pyrolysis operation has been applied in many fields of energy catalysis and storage. The pyrolysis operation can change the status and structure of the materials to obtain corresponding targeted catalysts. In this review, Co-based compounds refer to material containing the active ingredient of cobalt element during the hydrogen generation of boron hydride. Illustratively, the pyrolysis operation in this review refers to the catalysts whose last step is achieved through calcination at a certain temperature in air or an inert atmosphere in a tube furnace or other pyrolysis devices. The pyrolysis treatment is an important step in the preparation of metal catalysts that are effective for promoting the hydrolysis reaction of boron hydride. Thus, in this review, detailed information on the hydrogen generation of boron hydride is provided, including the hydrogen generation in the Batch/Slurry-Bed reactor. The preparation of Co-based compounds derived from pyrolysis of organic metal precursors based on metal organic frameworks (MOF), supported,

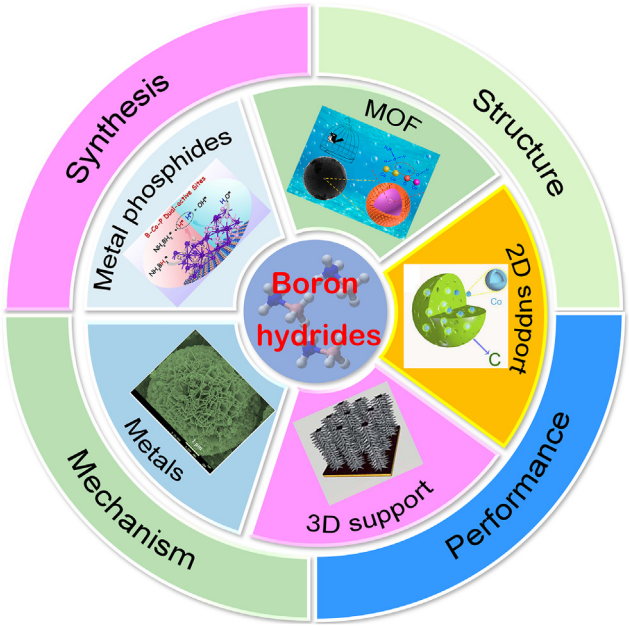

Figure 1. Schematic illustration of Co-based compounds derived from pyrolysis of organic metal precursors for hydrolysis of boron hydride

metal, and metal phosphide types are discussed in detail. Additionally, the corresponding characterizations and performance tests are summarized. Furthermore, four universal catalytic mechanisms for AB hydrolysis consisting of dissociation mechanism based on oxidative addition-reduction elimination, pre-activation mechanism, SN2 mechanism, four-membered ring mechanism, and acid-base mechanism are also investigated (Figure 1). Finally, prospects with remaining challenges are suggested based on the correlative literature reports about 2010–2023 presented in this review and summarized further outlooks in Co-based compounds derived from pyrolysis of organic metal precursor.

THE SUMMARIZATION OF BORON HYDRIDE

The excessive consumption of fossil fuels and corresponding environmental deterioration has triggered demand for sustainable and green energy. Hydrogen, as an ideal energy, has been generally deemed a promising candidate to replace conventional fossil fuels.[14] However, efficient and safe hydrogen storage and transportation technology are still one of the most restrictive challenges for improving the development of hydrogen economy.[25] Boron hydride as a chemical-solid hydrogen storage material is regarded as an ideal hydrogen source material for fuel cells because of its high hydrogen storage density and stable storage at room temperature. Illustratively, the general formula of the metal borohydride is $M(BH_4)_n$ (n refers to the valence status of metals). $M(BH_4)_n$ is the research focus of solid-state hydrogen storage materials because of the extremely high hydrogen storage capacity.[26,27] Currently, hydrogen carriers, such as AB,[28] sodium borohydride ($NaBH_4$),[13] formic acid (FA),[29] and hydrous hydrazine ($N_2H_4BH_3$),[30,31] have received intensive attention owing to their unique advantages. Among them, AB and $NaBH_4$ have been certified to be a convenient and safe liquid hydrogen carrier for portable hydrogen storage technology and have many presented research.[32]

Ammonia borane (NH_3BH_3, AB)

AB is a colorless molecular crystal under ambient conditions with a density of 0.74 g cm^{-3} and is soluble in water and other relatively polar solvents. The hydrogen stored in AB can be released either by thermolysis in a solid state and nonaqueous medium or metal-catalyzed reactions in protic solvents (water and methanol). Thermal decomposition of AB usually requires high temperature and the reaction was relatively difficult to control. In contrast, catalytic hydrolysis or methanolysis can provide a more convenient strategy for hydrogen generation from AB. AB as the simplest borane-nitrogen (B—N) compound, is a stable and environmentally sustainable material with impressive gravimetric and volumetric hydrogen density (19.6 wt % and 0.145 kg H_2 L^{-1}) and low molecular weight (30.86 g mol^{-1}).[3] AB is well ahead of the 2015 target for U.S. Departments of Energy (DOE) (9.0 wt % and 0.082 kg H_2 L^{-1}), making it the most attractive storage medium of all chemical hydrides.[33] More importantly, it can release high-purity hydrogen via an ambient temperature hydrolysis reaction in the presence of suitable catalysts. Three moles of hydrogen can be generated from one mole of AB through a complete hydrolysis reaction only in the presence of a suitable catalyst at ambient temperature. The hydrolytic cleavage of the AB complex is expounded as follows,[34,35]

$$NH_3BH_3 + 4CH_3OH \rightarrow NH_4B\text{–}(OCH_3)_4 + 3H_2 \quad \text{(Equation 1)}$$

$$NH_3BH_3 + 2H_2O \rightarrow NH_4BO_2 + 3H_2 \quad \text{(Equation 2)}$$

Compared to AB hydrolysis, AB methanolysis has several benefits. First, ammonia gas will not be produced during the process of AB methanolysis, which is favorable for the hydrogen-oxygen fuel cell. Second, $NH_4B(OCH_3)_4$ generated during AB methanolysis can be easily converted back to AB at room temperature by a chemical reaction, which makes AB renewable and can remarkably lower the overall cost of this technology. Third, due to the low freezing point of methanol (lower than −90°C), AB methanolysis technology can be applied to produce hydrogen at very low temperatures, which is extremely important in cold areas.[34] However, the hydrolysis of AB has been researched extensively because of the ease of analyzing the catalytic mechanism. Thus, much work has been done in the field of hydrogen generation.

Sodium borohydride ($NaBH_4$)

Sodium borohydride ($NaBH_4$) is discovered by H. C. Brown and his boss Schlesinger at the university of Chicago in 1942. $NaBH_4$ can remain stable at room temperature and atmospheric pressure. $NaBH_4$ breaks down quickly in acidic conditions to release hydrogen, so it can not react in acidic conditions, however, $NaBH_4$ can contact carboxylic acids in alkaline conditions to break down hydrogen quickly. $NaBH_4$ has been given high expectations for its high hydrogen storage capacity (10.8 wt. %), purity of hydrogen product stream, and stability in alkaline solution. From the stoichiometry of this reaction, 1 mol $NaBH_4$ can produce 4 mol H_2 under ambient conditions, which is much more efficient than other reported hydrogen storage materials. Hydrogen can be released through the hydrolysis of $NaBH_4$ according to the following equation,

$$BH_4^-(aq) + 4H_2O(l) \rightarrow B(OH)_4^-(aq) + 4H_2(g) \quad \text{(Equation 3)}$$

The above reaction occurs at room temperature, but the reaction rate is slow and needs an appropriate catalyst to enhance and regulate the catalysts. The main choices for $NaBH_4$ hydrolysis are acid and transition metal-based catalysts. When the acid medium is used as a catalyst, it is rather demanding for the reactor vessel during the reaction. Therefore, the transition metal-based catalysts have been considered more promising in enhancing the catalytic activity.

EVALUATION PARAMETERS ON HYDROGEN GENERATION

The hydrogen generation reaction system is different because of various boron hydrides, such as in our recent study, NaOH as a cocatalyst is applied in AB hydrolysis, Coincidentally, NaOH acts as a hindrance in the hydrolysis of $NaBH_4$. All the hydrogen generation materials have different approaches but equally satisfactory results. The hydrolysis of boron hydride was all performed through a water displacement method. The quality of the catalyst and the corresponding other value can increase or decrease according to the changes based on same magnitude. Each research group does something different when it comes to the hydrogen generation from boron hydride. Illustratively, through different measures, the reaction parameter and activity indicator can be achieved. Herein, AB is just an example to introduce in detail the producing hydrogen and provide some guidance for the scientific researcher.

Hydrogen generation in the batch reactor

The hydrogen generation in the batch reactor has many different test detailed operations for the water displacement method.[13,14,36–38] Namely, (1) Catalyst (20 mg) was preloaded into a round-bottom flask (50 mL). Then NaOH solution (1 M, 10 mL) containing AB (84 mg) was rapidly injected into the flask using a gastight syringe. A gas burette (200 mL) filled with water connected to the other side of the reaction flask was employed to collect the gas. The experiment was conducted by using a constant-temperature magnetic stirring apparatus, and the stirring speed was kept at 500 rpm.

Furthermore, the hydrolytic dehydrogenation experiments were performed in a two-necked round-bottom flask, in which one neck was sealed with a rubber cap, while the other was connected to a gas burette. We used a constant-temperature bath to maintain the reaction temperature of system. Certain amounts of catalysts were placed in the two-necked round-bottomed flask, and then AB solution was quickly injected using a syringe. The generated hydrogen in the system was identified though a gas chromatograph. And then record the amount of gas.[32]

Hydrogen generation in the slurry bed reactor

The continuous hydrolysis of AB was also tested through a water displacement method. Catalyst (20 mg) and water (80 mL) were placed into a glass slurry-bed reactor (100 mL) fixed on a magnetic stirrer. The NaOH (1 M) aqueous solution of AB (0.136 or 0.272 M, 60 mL) was put into the reactor bottom through an entrance at a flow rate of 1.20 mL min^{-1} by an injector pump. The mixture exited from the reactor top through an export tube and the stirring rate was fixed at 500 rpm. Hydrogen left the reactor through a top tube and its volume was measured in the same inverted and water-filled gas burette in a water-filled vessel.

Illustratively, for the above-mentioned hydrolysis process, the operation of the existence of NaOH or not has the ability to interpret the role of NaOH. The amounts of various materials can change in an equal proportion to conduct the hydrolysis of borohydride. And the nature of the reaction has no change. We can change the parameter of the reaction to adjust and improve the process of hydrogen generation.

Hydrogen generation activity descriptor

In catalytic reactions, the hydrogen generation rate is an indicator to measure the catalytic activity of materials. The volume or mole of hydrogen produced per unit of time is based on the elemental content of the active substance. Herein, the active material element is used as an example to illustrate the calculation of hydrogen generation rate in detail. In this review, the Co as an example in the calculation of active substance was used to assess the catalytic activity. The whole calculation format is listed in the following and the practical implications have some similar in a sense.

Hydrogen generation specific rate

The hydrogen generation-specific rate was calculated using the information from the stabilizing stages. The stabilizing stages refer to the stable phase of the hydrogen generation. Such as, the stabilizing stages present as follows, namely, 80 mL of hydrogen generated refers to the amount volume of hydrogen in a stable phase toward hydrogen generation and this principle helps to determine the volume of the calculation rate perfectly according to the following formula,[13,38]

$$r_B = \frac{80(mL)}{[t_{140} - t_{60}](min) * W_c(g)} \quad \text{(Equation 4)}$$

Here, r_B is the hydrogen generation specific rate; t_{140} and t_{60} represents the time of hydrogen generation for 140 mL and 60 mL, respectively; *Wc* is the weight of active substance of Co in the catalysts. Illustratively, the hydrogen volume will change with the change of the stability period during the catalytic reaction.

Turn over frequency

Another common method of rate calculation is the turn over frequency (TOF) value in this dehydrogenation reaction, TOF refers to the number of moles of hydrogen produced per mole of active material per unit time, h^{-1} and min^{-1} are the most common units. TOF (h^{-1}) was calculated through the following formula,[3,39]

$$\mathrm{TOF} = \frac{dn_{H2}}{n_{Co} * dt} \quad \text{(Equation 5)}$$

Herein, n_{H2} is the moles of generated hydrogen during the stability period of hydrogen generation process, while n_{Co} is the total moles of active Co in the sample, t is the reaction time in units of hours during the stability period. The unit of TOF is h^{-1}.

The different research has different calculation formats. The TOF also reported was based on the total amount of active metals. The equation of TOF calculation is given below,[15]

$$\mathrm{TOF} = \frac{dV_{H2}}{22.4 * V_s * C_{ca} * dt} \quad \text{(Equation 6)}$$

Here, V_{H2} was the total volume of hydrogen generated, V_s was the volume of solution (10 mL in this report), C_{ca} was the concentration of active metals in the catalyst, and t was the time for the completion of the reaction. Additionally, the TOF value reported also can be calculated using the following Equation 7,[36]

$$\mathrm{TOF} = \frac{dmol_{H2}(released)}{mol_{catalyst} * dreaction\ time\ (min)} \quad \text{(Equation 7)}$$

The TOF value reported in Equation 7 could be calculated from three parallel tests. (Caution, the err bar<2%).

Durability test

The durability plays a key role in the development of heterogeneous catalysis and the excellent stability is beneficial to realize the industrial applications. The measurement of the stability during the process of hydrogen generation is narrated as follows: The catalyst was collected after reacting one cycle following an operation of dry. According to the experimental operation of the hydrogen generation, the same producers repeated many cycles (at least 5 cycles for non-noble metal-based catalysts and 10 cycles for noble metal-based catalysts). Additionally, the other method is that after the completion of first cycle reaction, another AB solution was directly injected into the reaction system for the next run. This operation was repeated many cycles to assess the stability of the prepared catalysts.[15]

CATALYSTS DERIVED FROM DIFFERENT PRECURSORS

The precursor selection is important for the preparation and activity enhancement of targeted catalysts. The morphology, particle sizes, specific surface area and so on of precursors is the main physical and chemical indicators. The calcination temperature and calcination time are important factors affecting the properties of targeted materials. For the Co-based materials, different precursors can generate different structures and influence the catalytic activity. Thus, the Co-based compounds derived from pyrolysis of different organic metal precursor are classified in this review according to the different types.

MOFs precursors

MOFs are attracting increasing attention as a kind of material composed of metal ions and organic ligands with porous crystalline structures. MOFs possess adjustable and diverse ordered skeletal structures with modifiable surfaces. Moreover, MOFs can be used as adsorbents in gas adsorption and separation and as supports for metal NPs in heterogeneous catalysis. In recent years, MOFs have been used to prepare some porous carbon materials with a high specific surface area through metal-catalyzed thermal pyrolysis. The generated confining effect of organic ligands because of their highly porous ordered structure can be tentatively applied into energy conversion and storage areas. Some new nanostructures composed of metal or metal oxide and carbon matrix or carbon shells can be prepared from MOFs after thermal treatments. Additionally, MOFs with controllable shapes and high carbon contents can be used to make core-shell structures through thermal pyrolysis and these synthesized core-shell structures consisting of shells derived from organic ligands and metal or metal oxide cores can improve performances. Generally, the metals or metal oxides NPs generated from metal ions will be covered with closed or open carbon layer shells from organic ligands in thermal pyrolysis and the existence of core-shell will prevent the NPs from growing indefinitely and aggregation, which have a significant influence on catalytic activity.

The direct pyrolysis of MOF to obtain carbon-modified catalyst and the carbon can prevent the agglomeration of the NPs, thus endowing excellent catalytic activity. Carbon-coated cobalt nanosheets (Co@C) catalyst was designed using Co-MOF as the self-sacrificing template and starting a pyrolysis treatment of MOF precursor. The Co NPs are highly dispersed and encapsulated in porous carbon. At the pyrolysis temperature of 700°C, the obtained Co@C-700 catalyst exhibits optimal activity among the Co@C catalysts compared to the other prepared catalysts at different carbonization temperatures and retains 93.1% of its initial catalytic activity after five cycles in $NaBH_4$ hydrolysis[40] (Figure 2A). Porous magnetic cobalt/carbon composite (MCCC) via one-step carbonization of cobalt-based zeolitic imidazolate framework (ZIF-67) was synthesized and shows a superior catalytic capability with significantly low activation energy (25.8 kJ mol^{-1}) in $NaBH_4$ hydrolysis[41] (Figure 2B). Illustratively, through changing the carbonization temperatures during the pyrolysis under inert or others to optimize the catalytic activity without changing the composition. The use of different ligands has different effects on the chemical composition and can adjust the active structure in the catalyst. Noteworthily, during the preparation of the MOF precursors using the 2-methylimidazole and other organic ligands containing the N element, the N-modified carbon can be achieved in the process of the MOF pyrolysis. Based on this, nitrogen-doped porous carbon nanowires (NPCNW) were synthesized, and synchronously the generation of cobalt NPs was supported on the nitrogen-doped porous carbon (Co/NPCNW) via the one-step carbonization of Co-MOF. The N element is derived from the organic ligand of 1,3,5-benzene tricarboxylic acid and 4,4′-bipyridine. The prepared catalyst Co/NPCNW presents a hydrogen generation rate of 2638 mL min^{-1} g^{-1} and a relatively low activation energy of 25.4 kJ mol^{-1} in hydrolysis of AB[42] (Figure 2C). In conclusion, the rational design of catalyst precursors, such as the addition of some non-metal elements, can provide the research basis for AB hydrolysis in hydrogen storage applications.

The introduction of the second metal into the MOFs can change the chemical features and environments after the treatment of pyrolysis. Gao et al.[43] successfully prepared the bimetallic ZnCo-MOFs using the 2-methylimidazole as the ligands, cobalt nanoparticles packaged into N-doped porous carbon derived from the pyrolysis of MOFs. The catalyst showed excellent catalytic activity with a hydrogen generation rate of 1807 mL_{H2} min^{-1} $g_{Co}{}^{-1}$ and lower activation energy (20 kJ mol^{-1}) in the hydrolysis of $NaBH_4$ because of the contribution of highly dispersed Co nanoparticles and confinement effect. Additionally, the stability test confirmed that the deactivation of the catalyst was due to the deposition of borate species at the surface of the catalyst. The addition of Zn in MOFs as a "fence" expanded the distance of adjacent Co atoms in space and simultaneously the leaving Zn^{2+} sites generated free N sites during pyrolysis. The modification method allows the cobalt nanoparticles have a uniform and fine confinement within the porous carbon. This observation may provide an idea to modify and upgrade the stability of the catalyst (Figure 2D). Moreover, the Zn ion as a sacrificial agent can be removed from the catalyst when the temperature is as high as 800°C and is beneficial to reduce the sizes of NPs and enhance the dispersity of active sites. The above-mentioned strategies can apply to the other field for the construction of active structure.

Some modification of the other coating layer into the MOF precursor is essential for the improvement of activity and stability. Chen et al.[44] reported the synthesis of SiO_2-encompassed Co@N-doped porous carbon assemblies as a new type of recyclable catalyst for the calcination of ZIF-67@SiO_2 microtubes at high temperatures under an N_2 atmosphere. The surface layer of SiO_2 in the precursor microtubes is essential for the production of efficient catalysts by supplying an additional surface for Co nanoparticle to reduce their size. In addition, the SiO_2 layer renders a highly ordered arrangement of Co@N-doped porous carbon within the catalysts, possibly allowing the ease of mass transfer of AB within the catalysts. The optimized catalysts obtained via calcination at 800°C show remarkable catalytic benefits, including a high hydrogen generation rate of 8.4 mol min^{-1} $mol_{Co}{}^{-1}$, a relatively low activation energy of 36.1 kJ mol^{-1}, and remarkable reusability (at least 10 times). The results can provide new insight into the design and synthesis of highly ordered SiO_2-supported catalysts for different reactions (Figure 2E).

Particularly, the rational construction of heterogeneous interfaces is an effective way to adjust the electron distribution with rich active sites, and to optimize the chemisorption capacity of the catalyst, thus resulting in excellent catalytic efficiency. The combination of MOFs pyrolysis and controllable oxidation to generate the synergistic effect is important for the enhancement of hydrogen generation. Liu et al. reported a core-shell heterostructure of Co-Co_3O_4@C-n prepared via pyrolysis of Co-MOFs@glucose polymer and partial oxidation in the air (Figure 2F). During $NaBH_4$ hydrolysis, as-fabricated Co-Co_3O_4@C-n exhibited higher catalytic activity (5360 mL min^{-1} $g_{Co}{}^{-1}$) because of the synergistic interactions between Co and Co_3O_4 NPs.[13] The assembly-pyrolysis-oxidation strategy provides theoretical guidance in the design of novel nanocomposites. Xing et al.[45] reported Co-MOFs used as pyrolysis precursors to synthesize multilayer core-shell composites loaded on reduced graphene oxide (rGO) sheets and then used in $NaBH_4$ hydrolysis. Due to the encapsulation of multilayer core-shell structure, the shell plays a limiting effect on the core, prevent active components of catalysts aggregation, making the catalyst more stable. The core-shell structure features the multifunctionality in the regulation of surface structure and electronic properties, thus, increasing the catalytic activity.

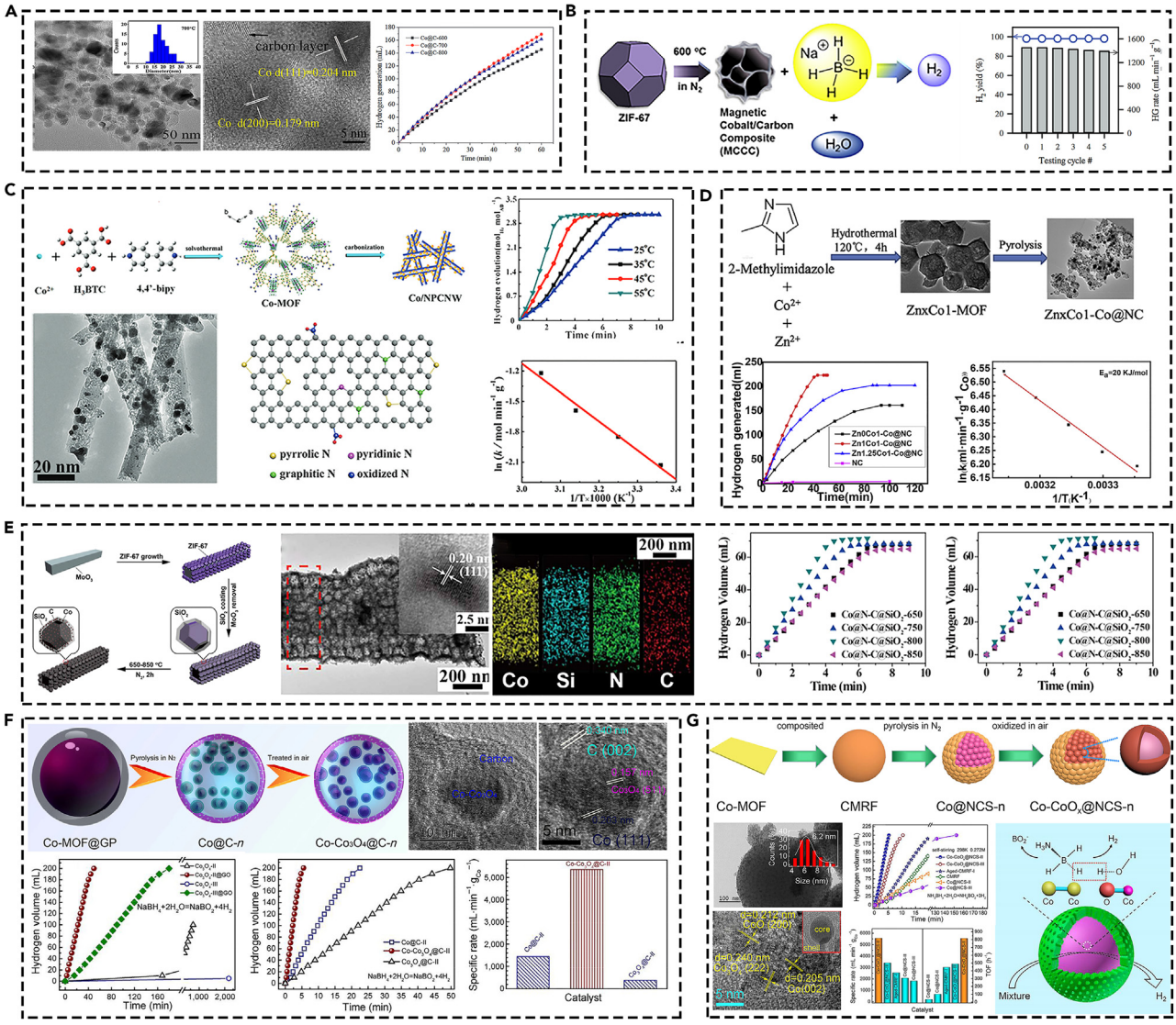

Figure 2. The analysis of structure and catalytic activity of Co-based catalysts on different MOFs

The analysis of structure and catalytic activity of (A) Co@C catalyst. Reproduced with permission,[40] Copyright 2016, Elsevier.
(B) Porous magnetic cobalt/carbon composite (MCCC). Reproduced with permission,[41] Copyright 2016, Elsevier.
(C) Co/NPCNW. Reproduced with permission,[42] Copyright 2017, Royal Society of Chemistry.
(D) Zn_xCo_{1-x}@NC. Reproduced with permission,[43] Copyright 2019, Elsevier.
(E) SiO_2-encompassed Co@N-doped porous carbon. Reproduced with permission,[44] Copyright 2019, American Chemical Society.
(F) Co-Co_3O_4@C-n series catalyst. Reproduced with permission,[13] Copyright 2017, Springer.
(G) Co-CoO_x@NCS-II series catalyst.[38] Copyright 2019, American Chemical Society.

The controllable oxidation of Co to CoO_x anchored onto the surface of rGO sheets makes a high hydrogen generation specific rate of 5560 mL min^{-1} g_{Co}^{-1}. Coincidentally, Co-N-doped carbon spherical catalysts (Co@NCS) were synthesized via the composition of Co-metal-organic frameworks and resorcinol-formaldehyde resin (CMRF) following precursor pyrolysis by Zhang et al.[38] Similarly, controllable oxidation of Co@NCS-n was also processed to obtain Co-CoO_x@NCS-II. The optimal catalyst demonstrated a superior specific hydrogen generation rate of 5562 mL min^{-1} g_{Co}^{-1} in AB hydrolysis because of the synergistic effect between Co and CoO_x (Figure 2G). Illustratively, the generation of core-shell structures was obtained by the formation of cores from metal ions and carbon shells from carbonization of ligands during the pyrolysis of MOFs precursors. The core-shell structure can prevent the agglomeration of metal NPs. The formation of the hetero-structure derived from the pyrolysis of MOF-based precursors adjusts the electronic character and thus enhance the catalytic activity. And the construction of the hetero-structure derived from MOFs can be used in the other transition metals according to the rational design of the active sites

based on the catalysis reaction. These synthetic strategies may improve the development and application of noble-metal-free catalysts in the sustainable catalysis field.

In a nutshell, the catalysts derived from the MOFs, the magnetism, porosity, and suitable size of cobalt-based active structure make MOFs became a promising synthesis method for the preparation of the catalysts and used for hydrogen generation. The MOFs also can be used in other catalysis fields. The carbon derived from the pyrolysis of MOFs is responsible for the stability during the hydrolysis of boron hydride. Furthermore, some modifications on MOFs precursors can be operated to enhance the improvement of the activity and stability. After the operation of the pyrolysis treatment on MOFs, some other operations such as introducing other metal or non-metal elements into catalysts to regulate the electronic structure are central to the design of the high-efficiency catalysts.

Supported precursors

Metal NPs are fundamental components of various catalysts because of their unique controllable size, morphology, and composition. The suitable NPs feature the advantages of small size, high surface atomic ratio, coordination unsaturation, and exposure a large number of active sites, thus expressing outstanding performance in heterogeneous catalysis and significantly increasing the effective utilization and scope of use. However, the problems of agglomeration and difficult separation of NPs after the reaction severely impede their practical application. Based on this, supported metal catalysts are an important class of multiphase catalysts and have widespread applications in the field of chemical industry. When the catalytic metal species are deposited on the support or modified on the support, the two-dimensional (2D) metal-support interface will naturally form. The generated interface holds the promise of effectively regulating the adsorption behavior of reactant intermediates or products on different chemical components, thus providing an opportunity to break the linear scaling relationship and improve the catalytic performance. The presence of suitable supports can avoid the agglomeration of NPs and make them disperse evenly. The metal-support interfaces between metals and supports have been studied in catalytic applications because of their significance in structural stability and efficient catalytic activity.[46–48] The construction of such a new interfacial structure for molecule activation holds great promise in many catalytic systems.[47] Through the process of pyrolysis, the supported catalysts present excellent catalytic activity in expediting the hydrogen generation of boron hydride.

Two-dimensional supports precursors

Two-dimensional (2D) supports such as rGO, carbon, and others present excellent characteristics in designing catalysts with high-efficiency active sites.[49] 2D materials have received extensive attention in various fields because of their 2D morphology and unique physical and chemical properties.[50] In detail, the rGO nanosheet as support was operated to design Co@g-C_3N_4-rGO catalyst through hydrothermal and pyrolysis strategy[51] (Figure 3A). In the process of catalyst preparation, g-C_3N_4 shells protect Co NPs cores from aggregating or growing. The connection between Co NPs and rGO was strengthened by the g-C_3N_4 shells to prevent them from leaching or flowing away. For hydrogen generation from the hydrolysis of $NaBH_4$ or AB, the catalyst presents the highest r_B of 3560 mL min^{-1} g^{-1} at room temperature. The magnetism of Co NPs and the shape of rGO nanosheets convey effective momentum transfer in the external magnetic field. This idea of composite design and magnetic momentum transfer will be useful for the development of both hydrogen generation and multifunctional composite materials. The functionalized graphene is of significance for the application of graphene in solving current energy and environmental problems. Graphene-based hybrid materials including porous graphene (PG) and carbon nanofibers anchored graphene oxide (GCNFs) through a controllable solid-phase reaction strategy were designed[52] (Figure 3B). The PG and GCNFs were formed through red-ox reaction between graphene and Co_3O_4 during the process of calcination. During the $NaBH_4$ hydrolysis, CoO_x NCs anchored onto PG and GCNFs provided hydrogen generation specific rates of 1472 mL min^{-1} $g_{Co}{}^{-1}$ and 2696 mL min^{-1} $g_{Co}{}^{-1}$, respectively. These outstanding catalytic activities are attributed to the synergistic effect of CoO_x NCs and PG/GCNFs. A *Pitaya pulp* structural cobalt-based carbon nanocatalyst through pyrolysis of the phenolic resin was obtained[53] (Figure 3C). The phenolic resin gradually decomposes into a carbon texture framework, while the metal complex turns into Co NPs. During hydrogen generation from the alkaline $NaBH_4$ and AB solutions, efficient catalytic performance of 3998 mL min^{-1} $g_{Co}{}^{-1}$ for $NaBH_4$ and 4677 mL min^{-1} $g_{Co}{}^{-1}$ for AB was achieved. Co nanoparticles fixed in the carbon matrix effectively prevent particles from aggregation and loss. The unique structure, its synergistic effects, and its self-stirring mode enable effective catalytic performance and good stability. Zhang et al.[54] used peanut shell as carbon precursor to synthesize porous sheet-like activated carbon in a fluidized bed and following a calcined in an N_2 flow at 450°C for 4 h (Zr/Co/C). This novel carbon-supported Zr/Co exhibits superior catalytic activity for the hydrolysis of $NaBH_4$ in alkaline medium (1708 mL min^{-1} g^{-1}) and following an activation energy of 34.84 kJ mol^{-1}. Zhu et al.[55] prepared colloidal carbon spheres (CCS) as a support to obtain cobalt catalysts (CCS/Co) for the first time through impregnation-chemical reduction method and following calcination in a tubular furnace under N_2 atmosphere at 673 K for 2 h. In particular, an average hydrogen generation rate of 10.4 L min^{-1} $g_{met}{}^{-1}$ is achieved at 20°C for CCS/Co with a Co loading content of 18.38 wt %. Zou et al.[56] synthesized highly dispersed Co-Ce-B nanoparticles supported on chitosan-derived carbon (Co-Ce-B/Chi-C) through chemical reduction and carbonization. A remarkably high hydrogen generation rate of 4760 mL min^{-1} g^{-1} at 30°C was achieved and followed by a low activation energy of 33.1 kJ mol^{-1} in $NaBH_4$ hydrolysis (Figure 3D). Co NPs embedded in porous N-doped carbon (Co@N-C) were fabricated through one-step thermolysis of Co(salen) at selected temperatures (600°C, 700°C, 800°C) under an Ar atmosphere.[57] The Co@N-C catalyst obtained at 700°C (Co@N-C-700) shows superior catalytic activity (TOF = 5.6 mol_{H2} $mol_{Co}{}^{-1}$ min^{-1}) and high sustainability with a 97.2% of its initial catalytic activity after 10 cycles during the hydrolysis of AB. Mahmood et al.[58] reported a 2D nitrogenated network polymer encapsulated cobalt-oxide (Co@C_2N) catalyst fabricated via an *in situ* solvothermal synthesis and following an annealing at 450°C under argon atmosphere for 2 h. Co@C_2N exhibits outstanding catalytic activities for hydrogen generation of 8903 mL min^{-1} g^{-1} at 303 K in hydrolysis of alkaline $NaBH_4$ (Figure 3E). Huang et al.[59] developed

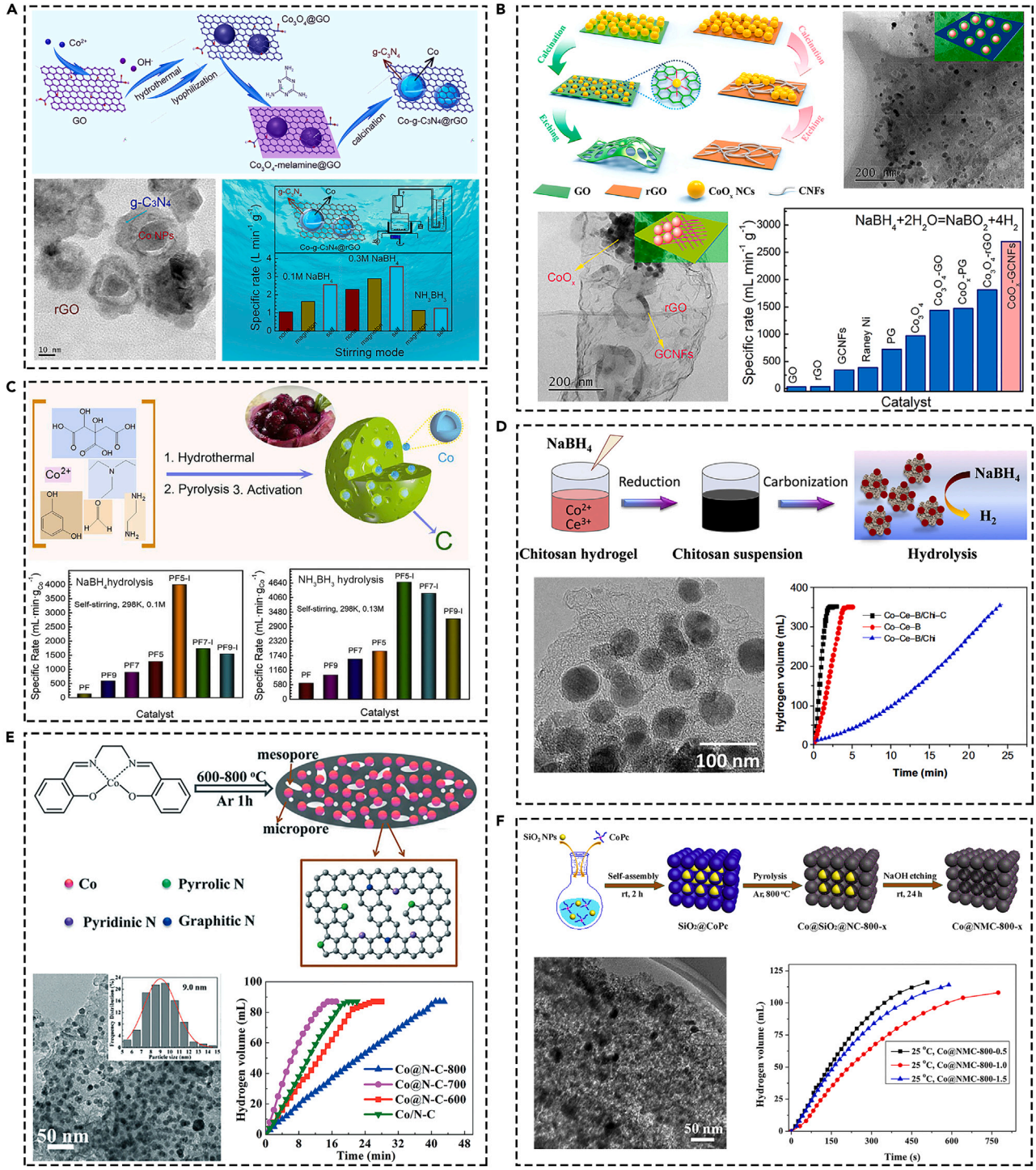

Figure 3. The analysis of structure and catalytic activity of Co-based catalysts on different 2D supports

(A) Co@g-C_3N_4-rGO catalyst. Reproduced with permission,[51] Copyright 2016, American Chemical Society.

(B) CoO_x-PG and CoO_x-GCNFs. Reproduced with permission,[52] Copyright 2018, American Chemical Society.

(C) PF-based catalysts. Reproduced with permission,[53] Copyright 2019, Elsevier.

(D) Co-Ce-B/Chi-C. Reproduced with permission,[56] Copyright 2018, Elsevier.

(E) Co@N-C. Reproduced with permission,[58] Copyright 2016, Royal Society of Chemistry.

(F) Co@NMC-800-0.5. Reproduced with permission,[61] Copyright 2016, Royal Society of Chemistry.

multiwalled carbon nanotubes supported cobalt-boron catalysts (Co–B/MWCNT) via the chemical reduction and pyrolysis in Ar atmosphere. The Co–B/MWCNT has a high rate of 5.1 L min^{-1} g^{-1} compared to 3.1 L min^{-1} g^{-1} on Co–B/C catalyst under the same conditions in hydrolysis of $NaBH_4$. Xu et al.[60] reported that mono-disperse cobalt NPs decorated on multi-walled carbon nanotubes (MWCNTs) were synthesized by an impregnation-reduction method and calcination of precursors and also used in the hydrolysis of AB. Zhang et al.[61] reported Co and nitrogen co-doped mesoporous carbon catalysts (Co@NMC-T-0.5, T represents the carbonization temperature (600°C–900°C), 0.5 indicates the weight ratio between cobalt phthalocyanine (CoPc) and SiO_2) synthesized via a facile and effective *in situ* mosaic strategy and annealing treatment (Figure 3F). Experimental results indicate that Co@NMC-800-0.5 exhibits the highest catalytic activity for the hydrolysis of AB among all the synthesized catalysts, which can be attributed to the superhigh surface area, pore volume, and large pore size of the support, as well as the modified electronic structure and chemical microenvironment of the metallic Co NPs. Fan et al.[62] successfully synthesized non-noble bimetallic CoNi NPs encapsulated within *h*-BN (CoNi@*h*-BN) via annealing freshly prepared metal ammine boride complexes [$Co_{0.5}Ni_{0.5}(NH3)_6]Cl_3$)/$NH_4BO_2$ and KBH_4 under flowing nitrogen gas at 900°C for 2 h. The result showed that CoNi NPs with a general size of 17 nm were completely encapsulated by *h*-BN shells, and the *h*-BN shells on the CoNi NPs are 10–20 layers. The obtained CoNi@*h*-BN demonstrated high sustainability, good stability (92% retained activity at reuse even recycled 5 times) and outstanding catalytic activity (176.19 mL min^{-1} $^{g-1}$ at 293 K) on hydrolysis of AB and a lower activation energy (E_a) of 28 kJ mol^{-1}. Additionally, the mesoporous silica, including beta zeolite seeded MCM-type was as the support to synthesize the corresponding catalysts. Zeolite-supported metal nanocatalysts have emerged as an indispensable class of industrial catalysts because of their superior catalytic activity and excellent stability, which are widely used in diverse catalytic conversions, such as hydrogenations, dehydrogenations, and reforming reactions.[63] Co catalysts supported on MCM41 (Co/MCM41) via simple pyrolysis at 550°C was obtained.[64] The effect of cobalt loading and weight percent of MCM41 on the catalytic activity was also investigated. The catalyst with the Co loading of 0.5 wt % (Co/MCM41-0.5w) exhibited the highest catalytic activity (915.2 mL_{H2} min^{-1} $g_{cat}{}^{-1}$) over all investigated catalysts in $NaBH_4$ hydrolysis. Moreover, the different pyrolysis temperatures of 350°C and 650°C were also studied and the results indicated that the 550°C presented excellent performance. Just like discussed in the above results, the different pyrolysis temperatures can influence the micro-chemical structure and thus regulate the catalytic activity of catalysts. Luo et al.[65] reported cobalt boride catalysts are supported on modified MCM-41 (Co@M41S) via chemical adsorption and then pyrolyzed at 540°C for 3 h. The Co@M41S presented excellent activity (258 L min^{-1} $mol_{Co}{}^{-1}$) in AB hydrolysis reactions, which is better than traditional Co@M41T (73.4 L min^{-1} $mol_{Co}{}^{-1}$). Illustratively, the supports of metal oxides were also investigated to prepare the Co-based catalysts for enhancing the catalytic activity of hydrogen generation. Al_2O_3 as the support to obtain Co/Al_2O_3 catalyst was successfully designed through impregnation-chemical reduction method and calcination treatment under nitrogen atmosphere at different temperatures. The catalyst was used to catalyze the methanolysis of $NaBH_4$ for hydrogen generation.[66] A novel catalyst Ti-supported nanostructured $MnCo_2O_4$ film was developed through hydrothermal reaction and calcination at 400°C for 3 h. In hydrolysis of AB, the catalyst conveyed a TOF of 24.3 min^{-1} and with an excellent stability of 96% even after long-time usage.[67]

In a nutshell, the 2D supports such as carbon-based or other elemental modifications hold promise in designing the supported catalysts with high-efficiency active sites to enhance the activity of hydrogen generation. However, challenges such as the construction of supported catalysts with high-efficiency catalytic active sites still exist in heterogeneous catalysis. Based on this, the monolithic catalysts play a crucial role in gas-solid phase reactions such as cracking/reforming, and catalytic oxidation/hydrogenation.[68–70]

Three-dimensional supports precursors

Copper foam, Ni foam, Ti mesh, carbon cloth, and so on have the advantages of special three-dimensional (3D) channels and good heat conduction performance have been widely considered in various catalyst carriers.[71] The 3D supports are also conducted to prepare Co-based catalysts through the pyrolysis treatment. Xie et al. reported cobalt oxide nanosheet array on carbon cloth (CoO/CC) and CuO/Co_3O_4 core-shell nanowires array on copper foam (CuO/Co_3O_4 core-shell NA/CF) catalysts obtained through pyrolysis of corresponding precursors.[72,73] The obtained catalysts presented excellent catalytic activity during the process of $NaBH_4$ hydrolysis (Figure 4A). Cui et al.[74] used the Ti mesh as the support to prepared cobalt carbonate hydroxide nanowire array on Ti mesh (CHNA/Ti) through hydrothermal and calcination in an Ar flow at 250°C for 2 h. Self-supported cobalt oxide nanorod array on a Ti sheet (Co_3O_4 NA/Ti) was obtained through calcination in air at 400°C for 2 h of Co(OH)F precursor.[75] The synthesized catalysts showed excellent activity with an activity of 1940 mL min^{-1} $g_{Co3O4}{}^{-1}$ in the dehydrogenation of $NaBH_4$. Dai et al.[76] prepared a Co-W-B amorphous catalyst supported on Ni foam (Co-W-B/Ni foam catalyst) using a modified electroless plating method. Subsequently, the Co-W-B/Ni foam catalysts were pyrolyzed at a temperature ranging from 100°C to 500°C for 2 h under pure Ar atmosphere and present highly effective for catalyzing hydrogen generation from alkaline $NaBH_4$ solution. The effect of different pyrolysis temperature on the hydrogen generation and the specific surface area was studied. The optimal catalyst presented excellent activity of 15 L min^{-1} $g_{(Co–W–B)}$ and with a lower activation energy of 29 kJ mol^{-1} (Figure 4B).

Generally, the catalysts can be prepared through facile one-pot solution reaction, pyrolysis at high temperatures, and oxidation in air. The various valence states of Co can be observed by utilizing various characterization methods. In a nutshell, the interface between active metal and support plays a key role in catalyzing various reactions. The design of efficient supported catalysts has been frontier research in catalysis field.[77] However, the catalytic properties of interfacial structures can be influenced by many factors, such as the size of active metals, the type of supports, and the strength of metal-support interactions, making targeted creation of active interfaces with specific structures a challenge.[78,79] Therefore, the construction of active interface is essential for the design of efficient supported catalysts. How to construct an efficient catalytic interface between metal and support has attracted widespread attention from researchers. It is generally believed that the interaction between metal and support is conducive to improving the dispersion of active metals, but there will also be cases of excessive

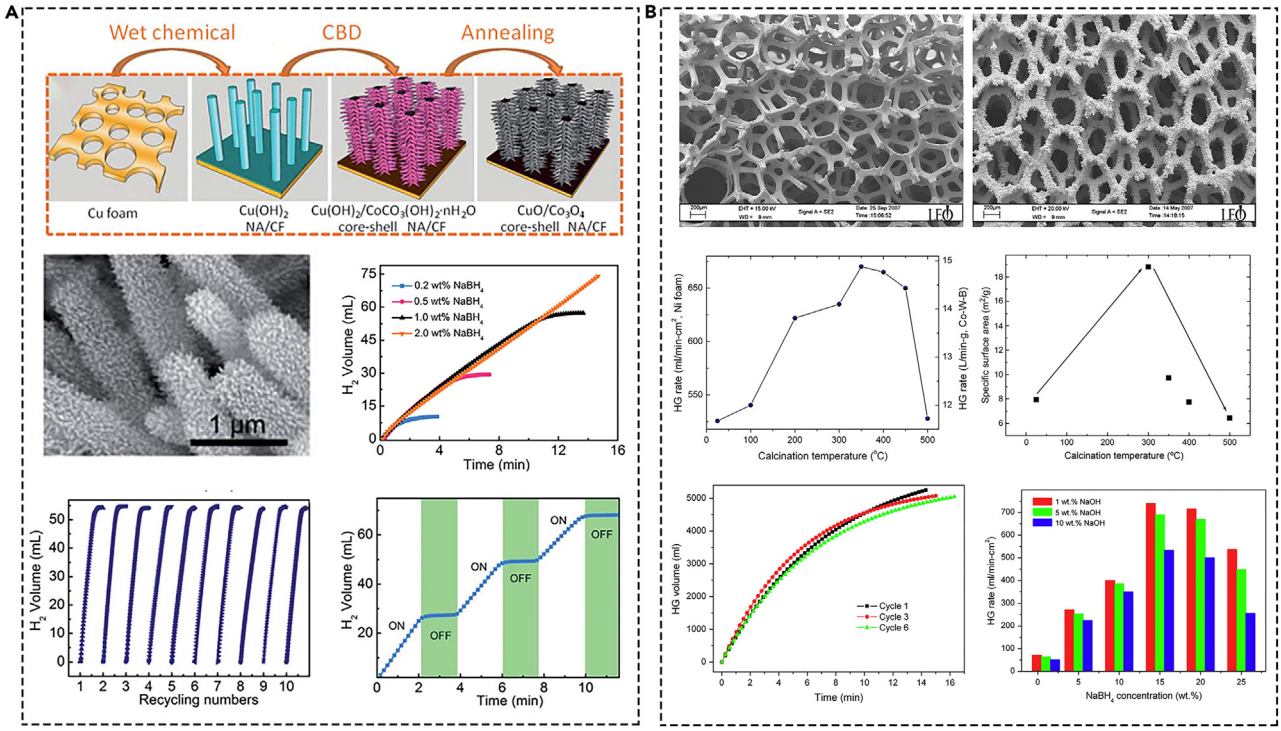

Figure 4. The analysis of structure and catalytic activity of Co-based monolithic catalysts on different 3D supports

(A) CuO/Co_3O_4 core-shell nanowires array on copper foam. Reproduced with permission,[73] Copyright 2016, Royal Society of Chemistry.

(B) Co–W–B/Ni foam. Reproduced with permission,[76] Copyright 2008, Elsevier.

coating, resulting in a large loss of active sites. Therefore, it is essential to properly design and control metal-support interactions to create rich and efficient interface sites for molecular transformation.[47] Additionally, supported metal catalysts are typical heterogeneous catalysts, and most supported metal catalysts have metal particle sizes at the nanoscale. Because of their special geometric structure and electronic properties of supported catalysts, the catalyst exhibits excellent catalytic properties. The problem is that when the metal particles are reduced to the sub-nanometer scale, their specific surface area increases sharply, resulting in a dramatical increase in the free energy of the metal surface. Additionally, the generated high surface energy in the process of catalyst preparation and reaction will make metal particles to agglomerate to form large clusters, resulting in catalyst inactivation. Therefore, excavating the single-atom catalysts have hails as a research hotspot thanks to their extremely high atomic utilization rate and relatively uniform active center.

Metal precursors

The Co-based catalysts obtained from pyrolysis of metal precursors were also reported and used in the hydrogen generation of boron hydride. Tomboc et al.[80] reported a synthesis of Co_3O_4 with porous macrocube structure through hydrothermal treatment of chitosan/urea/$Co(NO_3)_2$ $6H_2O$ mixtures at 180°C for 8 h and then calcined at different temperatures (500°C, 600°C, 700°C and 800°C) for 4 h. The catalyst showed a high hydrogen generation rate of 1497.55 ml_{H2} min^{-1} $g_{cat}{}^{-1}$ at 25°C. Durano et al.[81] developed a simple precipitation method to prepare Co_3O_4 nanorods using cobalt chloride and urea in aqueous solution and then following a calcined at 600°C, 700°C, 800°C for 4 h and used in $NaBH_4$ hydrolysis, which present an activity of 1776 ml_{H2} min^{-1} $g_{cat}{}^{-1}$. Figen et al.[82] reported a novel perspective Co-B catalysts prepared through sol-gel reaction of boron oxide (B_2O_3) with cobalt (II) chloride hexahydrate ($CoCl_2$ $6H_2O$) in the presence of citric acid ($C_6H_8O_7$) and then calcined at 500°C and 700°C. The maximum hydrogen generation rate is observed with an amorphous Co-B catalyst (9157.20 mL min^{-1} $g_{cat}{}^{-1}$) in hydrogen generation from AB and the corresponding activation energy (E_a) is only 47.50 kJ mol^{-1}. The Co or CoO_x as the active sites provide the responsibility for the absorption and dissociation of reactants thus expediting the catalytic activity. However, the single Co-based catalysts have the disadvantages of easy agglomeration and low activity, which dramatically decreases the activity of catalysts. Therefore, the investigation of the introduction of other metal or non-metal elements is beneficial for the enhancement of the catalytic activity.

Precise regulation of metallic NPs structure is essential to understand structure-activity relationships in catalytic reactions and improve catalytic performance. The introduction of other metal or non-metal elements can adjust the electronic structure and modify the chemical environment and thus construct new active sites to boost the catalytic reaction.[83] Zhang et al.[84] fabricated porous single-crystal CoO nanorods (PS CoO NRs) through gas phase cation exchange using ZnO NRs as a template. Additionally, the cation exchange was verified to proceed gradually from the outer surface to the inner core of ZnO NRs, and CoO NRs can be achieved at the exchange temperature of 600°C. The

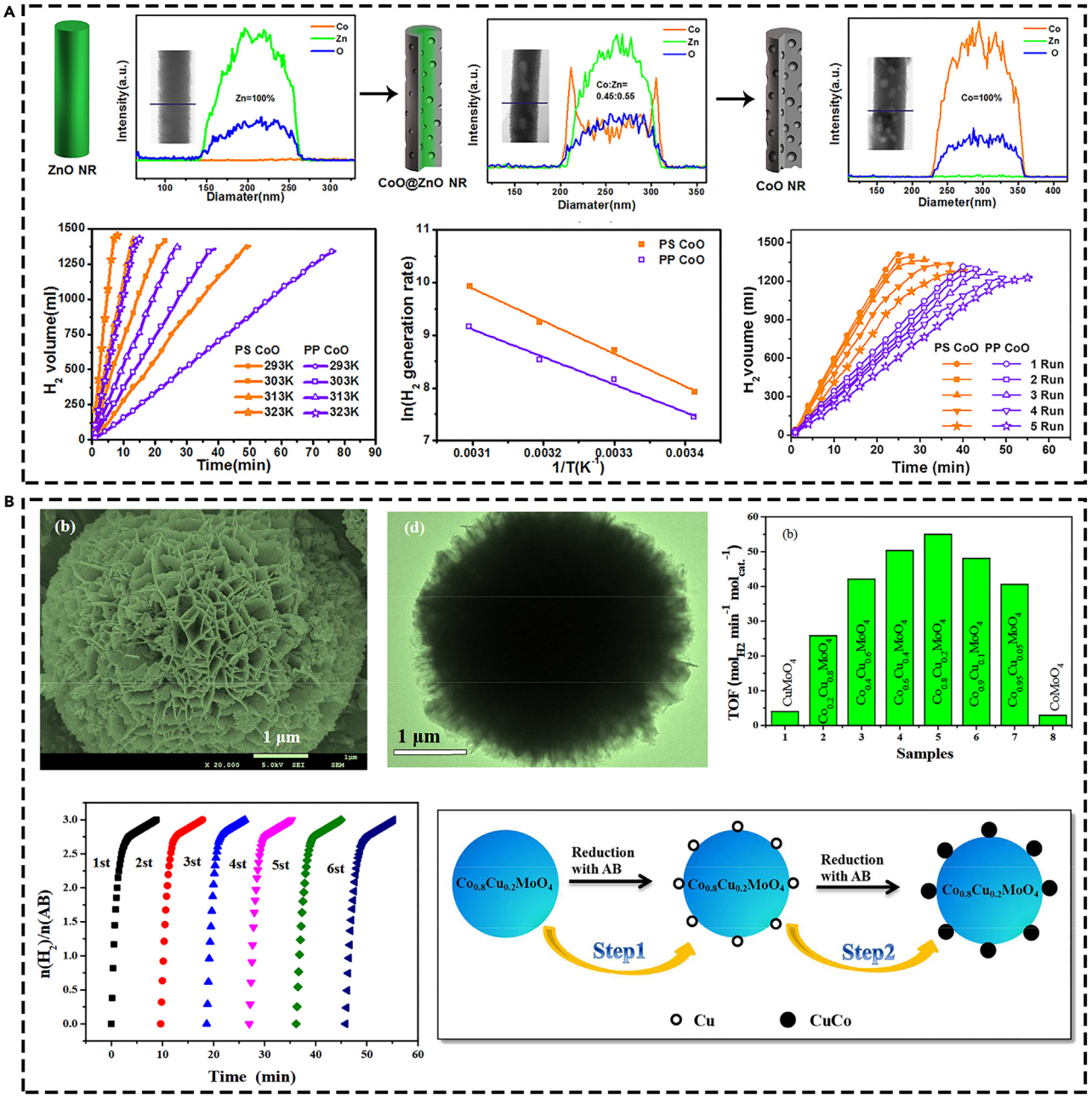

Figure 5. The analysis of the structure and catalytic activity of Co-based catalysts derived from the pyrolysis of metal precursors

(A) CoO NRs. Reproduced with permission,[84] Copyright 2017, American Chemical Society.

(B) $Co_{0.8}Cu_{0.2}MoO_4$. Reproduced with permission,[89] Copyright 2018, American Chemical Society.

single-crystal structure of the ZnO template is well-preserved after the cation exchange, and numerous nanopores form in the PS CoO NRs because of the volume shrinkage. As-synthesized PS CoO NRs exhibited outstanding catalytic activities for $NaBH_4$ hydrolysis in alkaline solutions with hydrogen generation rates of 20.3 L min^{-1} g^{-1} (Figure 5A). Wu et al.[85] synthesized a series of Ni-Co-B catalysts by a two-step technique, namely, chemical reduction (5% $NaBH_4$+1% NaOH) to prepare the precursors, and heat-treatment (573 K, 673 K, 773 K, 973 K) to adjust the crystal structures under the protection of an Ar atmosphere. The sample treated at 673 K achieves an average hydrogen generation rate of 708 mL min^{-1} g^{-1} in $NaBH_4$ hydrolysis, which can give successive hydrogen supply for a 115 W portable proton-exchange membrane fuel cell (PEMFC). Zhao et al.[86] reported various metal elements (M = Ni, Co, NiCo) dispersed on graphene oxide (GO) to form the M-GO hybrids through a facile method. The samples were heated to 300°C in H_2 (100 sccm) atmosphere at the rate of 8 °C min^{-1} and held at 300°C for 2 h. The hybrids showed good catalytic activities in the hydrolytic dehydrogenation of AB, which presented superior activity

compared to the metal NPs or GO alone. NiCo-GO shown the optimal TOF value of 6.78 min^{-1} and catalytic activity decreases but still has a value of about 65% after circulation. Barakat et al.[87] synthesized MnO-doped Co nanofibers using electrospinning technology. Briefly, electrospun nanofibers composed of poly(vinyl alcohol), cobalt acetate, and manganese acetate were vacuously dried and calcined in an Ar atmosphere at 850°C for 5 h, which was introduced as an effective catalysts for AB hydrolysis. Qian et al.[88] reported Co-Zn-S nano-porous microspheres catalyst synthesized through a solvothermal method and following an annealing treatment. The catalyst also showed good catalytic performance toward the hydrolysis of AB and produced around 70 mL of hydrogen. Liao et al.[89] prepared a series of $Co_xCu_{1-x}MoO_4$ microspheres through an annealing treatment at 500°C for 2 h. Especially, $Co_{0.8}Cu_{0.2}MoO_4$ exhibited excellent catalytic activity with a TOF of 55.0 min^{-1} toward AB hydrolysis (Figure 5B). Illustratively, the introduction of noble-metal holds the promise of improving catalytic activity due to its special d band center. For example, the introduction of Pd-doped Co-based catalysts synthesized through a calcination of precursors and used in the catalytic hydrolysis of AB.[66,90] However, the rare resource and prohibitive cost severely hampered their widespread application.

Metal phosphides precursors

Metal phosphides (MPs) have adjustable composition, excellent electrical conductivity, rich phase structure, and good redox performance have been used in catalysis field.[91–95] For the hydrolysis of boron hydride, the introduction of phosphorus (P) element can regulate the electronic structure and coordination environment, thus presenting great application potential in the fields of energy storage and heterogeneous catalysis.[96,97] The P regulation strategy is referred to introducing P atoms into the metal-based catalytic active center/active phase and forming an efficient active structure.[98,99] The incorporation of P atom can regulate the electronic structure, valence state, and existence form of the metal through the coordination strategy, thus helping to improve the catalytic reactivity of metal sites.[100] Although MPs have great potential, there are still many great challenges, such as, the lattice stress release caused by the replacement of P atoms leads to aggregation and sintering of catalysts in the process of P-inducing, thus destroying the original structure and reducing the catalytic activity of catalysts. Based on this, the construction of high-efficiency accessible active sites through rational regulation strategy of P atoms, and to understand the correlation between the active sites, the catalytic performance and catalytic mechanism of the catalysts are of great significance in the field of heterogeneous catalysis. Based on this, more research on MPs to improve the hydrogen generation of boron hydride is investigated. The atomic-bridge structure in B-Co-P dual-active sites on boron nitride nanosheet was rationally design through simple $NaBH_4$ reduction and P-inducing strategy, which present excellent activity during the catalytic hydrogen generation of AB.[2] The introduction of P atom regulates the chemical environment of Co and generates new active sites of Co-B and Co-P. The existence of the dual-active sites is responsible for the absorption and dissociation of the AB and H_2O molecule (Figure 6A). Additionally, CoBP nanoparticles supported on 3D nitrogen-doped graphene hydrogel was synthesized and conveyed superior catalytic activity for hydrogen generation from hydrolysis of AB.[101] Through the MOFs pyrolysis to obtain the corresponding MPs is the common method. Polar O-Co-P surface was prepared through the pyrolysis of compound precursors of Co-MOF and resorcinol-formaldehyde, the introduction of P atom changes the existence valence of Co and boosts the bimolecular activation in AB hydrolysis.[102] CoP nanoparticles encapsulated in carbonaceous nanorods (CoP@CNR),[103] hierarchical porous carbon (HPC)[104] derived from Co-MOF-74 and the corresponding phosphorization treatment under different treatment methods was obtained and convey excellent performance on the dehydrogenization of AB. Cobalt phosphide carbon-based nano-frameworks (CoP@CNFs) was obtained through Zn/Co-ZIF as the template combined with the pyrolysis treatment. Zn in the MOF precursor plays the dual crucial role of separating the Co ions and maintaining the framework during pyrolysis. The hierarchical porous structure, well-exposed active sites, and hydrophilic channels make the catalyst exhibited extraordinary TOF of 165.5 min^{-1} for hydrogen generation of AB[105] (Figure 6B). The Co-based bimetallic phosphides, especially NiCo-based phosphides were also studied and presented high activity. Through one-pot chemical reduction approach to synthesize ultrafine $Ni_{0.13}Co_{0.87}P$ nanoparticles on halloysite nanotubes and the catalyst presented a TOF of 47.5 min^{-1} in the hydrogen evolution from AB. The synergistic effect among Ni, Co, and P in $Ni_{0.13}Co_{0.87}P$ effectively enhances their interaction with AB and thus boost the activity[106] (Figure 6C). Additionally, CoNiP nanoboxes on graphene oxide (CoNiP/GO) were synthesized through pyrolysis and P-inducing strategy, which achieved a remarkable TOF value of 134.6 min^{-1} because of the slightly modulated chemical state of Co[107] (Figure 6D). Boron nitride–supported NiCoP nanoparticles were harvested via the hydrothermal-phosphorization strategy and presented a TOF of 86.5 min^{-1} in the hydrogen generation from AB, the synergistic effect between Ni, Co, and P, as well as the strong metal-support interaction between NiCoP and h-BN.[108] Uniformly dispersed $Co@Co_2P$ core-shell nanoparticles (NPs) embedded in N-doped carbon nanotube polyhedron ($Co@Co_2P$/N-CNP) were achieved through a carbonization-phosphidation strategy and afforded a high TOF value of 18.4 min^{-1} for hydrogen generation from AB. Benefiting from the electronic effect of P doping, high dispersibility and strong interfacial interaction between NPs and support endows the excellent activity[109] (Figure 6E). Moreover, the monolithic catalysts based on MPs were also fabricated. The self-supporting NiCoP supported on nickel foam was synthesized and presented excellent activity for hydrogen generation via hydrolysis of AB.[110] Cobalt phosphide nanowall arrays supported on carbon cloth presented a hydrogen generation rate of 5960 mL min^{-1} g_{CoP}^{-1} during the hydrolytic dehydrogenation of $NaBH_4$.[111] Self-supported CoP nanosheet arrays on Ti mesh (CoP/Ti mesh) were obtained and followed with a hydrogen generation rate of 6100 mL min^{-1} g_{CoP}^{-1} in alkaline $NaBH_4$ solution.[112] The introduction of low noble metal into Co-based catalysts can adjust the active structure of metal and thus boost the hydrogen generation. Pd@Co@P NPs with orange-like supported on rGO was designed through one-pot co-reduction synthesis. The synthesized catalyst presented excellent TOF of 127.57 min^{-1} for catalytic hydrolysis of AB because of the existence of an orange-like structure, good dispersion of Pd@Co@P/rGO NPs, and the synergistic electron interactions between palladium, cobalt, and phosphorus[113] (Figure 6F). The comparison of Co-based catalysts contain the typical catalysts are listed in Table 1.

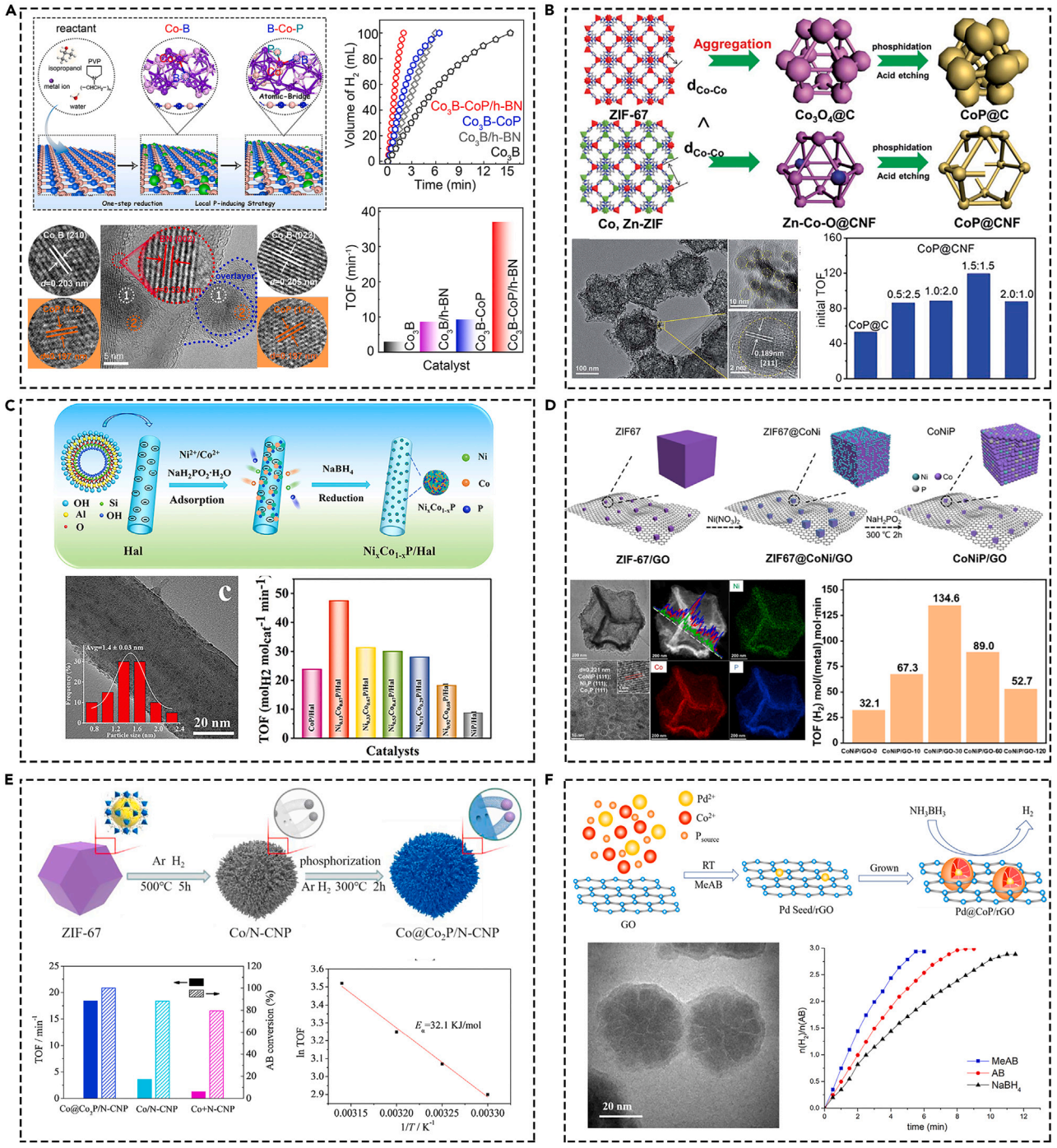

Figure 6. The analyses on the structure and catalytic activity of Co-based phosphides

(A) B-Co-P atomic structure. Reproduced with permission,[2] Copyright 2022, Elsevier.

(B) CoP@CNF. Reproduced with permission,[105] Copyright 2019, Royal Society of Chemistry.

(C) $Ni_xCo_{1-x}P$/Hal. Reproduced with permission,[106] Copyright 2021, Elsevier.

(D) CoNiP/GO. Reproduced with permission,[107] Copyright 2022, Elsevier.

(E) $Co@Co_2P$/N-CNP. Reproduced with permission,[109] Copyright 2021, Elsevier.

(F) Pd@Co@P/rGO. Reproduced with permission,[113] Copyright 2021, Elsevier.

Table 1. The comparison of Co-based catalysts contain the typical catalysts included in this review

Catalysts	Catalyst mass	Reactant	NaOH	Catalytic activity	E_a (kJ/mol)	Year	Reference
Co@C-700	10 mg	$NaBH_4$	yes	–	56.9	2019	Zhang et al. [40]
Co/C	–	$NaBH_4$	yes	1738[a]	25.8	2016	Lin et al.[41]
Co/NPCNW	10 mg	$NaBH_4$	no	2638[a]	25.4	2017	Zhou et al.[42]
Zn1Co1-Co@NC	10 mg	NaBH4	yes	1807[a]	20	2019	Gao et al.[43]
Co@N−C@SiO_2	10 mg	AB	no	8.4[a]	36.1	2019	Chen et al.[44]
Co-Co_3O_4@C-n	20 mg	$NaBH_4$	yes	5360[a]	37.12	2016	Liu et al.[13]
Co@CoO_x@N-CG	20 mg	$NaBH_4$	yes	5560[a]	36.6	2016	Liu et al.[13]
Co-CoO_x@NCS-II	20 mg	AB	yes	5562[a]	46.37	2019	Zhang et al.[38]
Co@g-C_3N_4-rGO	20 mg	$NaBH_4$	yes	3560[a]	35.42	2016	Duan et al.[51]
CoO_x/GCNFs	20 mg	$NaBH_4$	no	2696[a]	28.3	2018	Wu et al.[52]
Co-CoO_x/C	20 mg	AB	yes	4677[a]	30.84	2019	Wang et al.[53]
Zr/Co/C	–	$NaBH_4$	yes	1708[a]	34.84	2013	Zhang et al.[54]
CCS/Co	20 mg	$NaBH_4$	yes	10400[a]	24.04	2012	Zhu et al.[55]
Co-Ce-B/Chi-C	150 mg	$NaBH_4$	yes	4760[a]	33.1	2018	Zou et al.[56]
Co@N-C-700	20 mg	AB	no	5.6[a]	31.0	2016	Wang et al.[57]
Co@C_2N	10 mg	$NaBH_4$	yes	8903[a]	66.17	2015	Mahmood et al.[58]
Co–B/MWCNT	10 mg	$NaBH_4$	yes	5100[a]	40.4	2008	Huang et al.[59]
Co/CNT	20 mg	$NaBH_4$	yes	–	33.8	2012	Xu et al.[60]
Co@NMC-T-0.5	30 mg	AB	no	–	41.6	2018	Zhang et al.[61]
CoNi@h-BN	–	AB	–	176.19[a]	28	2017	Fan et al.[62]
Co/MCM41–0.5w	–	$NaBH_4$	yes	915.2[a]	108.7	2019	Shu et al.[64]
Co@M41S	–	$NaBH_4$	no	258[a]	54.6	2013	Luo et al.[65]
$MnCo_2O_4$ film	–	AB	yes	24.3[b]	17.5	2017	Liu et al.[67]
CHNA/Ti	–	$NaBH_4$	yes	4000[a]	39.78	2016	Cui et al.[74]
Co_3O_4 NA/Ti	–	$NaBH_4$	yes	1940[a]	59.84	2016	Huang et al.[75]
Co–W–B/Ni foam	–	$NaBH_4$	yes	15000[a]	29	2008	Dai et al.[76]
Co_3O_4	20 mg	$NaBH_4$	yes	1497.55[a]	47.97	2017	Tomboc et al.[80]
Co_3O_4 nanorods	–	$NaBH_4$	no	1776[a]	49.52	2017	Durano et al.[81]
Co-B	–	AB	–	9157.20[a]	47.5	2013	Kantürk et al.[82]
PS CoO NRs	10 mg	$NaBH_4$	yes	20333[a]	45.94	2015	Zhang et al.[84]
Ni–Co–B	100 mg	$NaBH_4$	yes	708[a]	–	2011	Wu et al.[85]
NiCo-GO	10 mg	AB	no	6.78[b]	–	2016	Zhao et al.[86]
$Co_xCu_{1-x}MoO_4$	10 mg	AB	yes	55.0[b]	39.6	2018	Liao et al.[89]
B-Co-P	10 mg	AB	yes	37[b]	51.8	2022	Zhang et al.[2]
$Co_{0.79}B_{0.15}P_{0.06}$/NGH	–	AB	no	32.8[b]	39.42	2018	Men et al.[101]
O-Co-P	20 mg	AB	yes	37[b]	41.0	2023	Zhang et al.[102]
CoP@CNR	10 mg	AB	yes	10014[a]	–	2021	Jiang et al.[103]
CoP@HPC	–	AB	–	27.7[b]	42.55	2020	Ma et al.[104]
CoP@CNFs	–	AB	yes	165.5[b]	–	2019	Hou et al.[105]
$Ni_{0.13}Co_{0.87}P$/Hal	–	AB	yes	47.5[b]	41.8	2021	Xiong et al.[106]
CoNiP/GO	5 mg	AB	yes	134.6[b]	44.12	2022	Chen et al.[107]
$Ni_{0.8}Co_{1.2}P$@h-BN	10 mg	AB	yes	86.5[b]	40.26	2019	Zhou et al.[108]
Co@Co_2P/N-CNP	–	AB	–	18.4[b]	32.1	2021	Wang et al.[109]
Co_2P nanosheets	–	AB	–	44.9[b]	32.03	2022	Wan et al.[128]

(*Continued on next page*)

Table 1. *Continued*

Catalysts	Catalyst mass	Reactant	NaOH	Catalytic activity	E_a (kJ/mol)	Year	Reference
CoP NAs/CC	–	AB	yes	5960[a]	42.1	2016	Yang et al.[111]
CoP/Ti mesh	0.6 mg	AB	yes	6100[a]	42.01	2016	Liu et al.[112]
Pd@Co@P/rGO	–	AB	–	127.57[b]	39.05	2021	Qu et al.[113]

Summarily, the enhancement of catalytic activity, stability, and the clearness of catalytic mechanism always are the key science problem during the construction of non-noble metal-based catalysts. The P atom regulation strategy plays a paramount role in synthesizing catalyst with high-efficiency active sites. Additionally, we can change the temperature of P-inducing, different types of phosphorus sources to design the catalysts with precise and controllable structures. At the same time, the introduction of special supports into the metal phosphide NPs and the migration of metal phosphide NPs on the supports through the activation of P atoms can accelerate the electron transfer. In addition, the regulation of P elements can regulate the chemical composition and electronic structure of the active phase of active structure, change the intrinsic characteristics of the catalysts, and then promote the catalytic reaction. Illustratively, through *in situ* spectrometric characterization and theoretical calculation can provide theoretical guidance for the design of highly active catalysts.

The interaction between cobalt and other components

From the above-mentioned types derived from different precursors, we can infer that different precursors have different effects on the structure formation of catalysts, thus influencing the activity of catalysts. Illustratively, the investigation of the interaction between cobalt and other components is important for understanding the nature of catalysts and thus revealing the catalytic mechanism. From the above-mentioned discussion, we can conclude that the introduction of other components can change the structure of catalysts, adjust the chemical valence and thus generate new active structures. The effect of other components on the catalytic activity of boron hydride can be divided into two types of effects: (1) The direct action, namely, the presence of the other components can generate a synergistic effect. The Co substance and the other components have the ability to activate the boron hydride and water molecules. The enhanced activity is contributed by the synergistic effect of them. (2) The indirect action. This refers to the introduction of other components that can affect the chemical coordination environment of Co through electronic promoter or structural promoter and so on. This operation can regulate the surface structure and electronic properties of Co, thus promoting the reaction activity. How the Co and the other components contribute to enhancing the activity still have vast space for research. Additionally, for the different detailed active substances, the activity and mechanism are different. The core research content for us is to construct high-efficiency active sites, clarify the origin of the improvement of catalytic activity and thus reveal the structure-activity relationship.

The comparison of other methods for obtaining catalysts

Besides the mentioned pyrolysis method, other methods are also used to synthesize catalysts and present excellent performance during the process of hydrogen generation. In this part, we will select representative research to present other methods for catalyst preparation. The other methods may provide guidance for the design and synthesis of catalysts for hydrogen generation. For example, the simple impregnation reduction method was applied to synthesize Ru/N-RHC (N-RHC: nitrogen-doped rice husk activated carbon support) catalysts, and present a TOF of 83.71 min^{-1}.[114] The existence of support can evenly disperse nanoparticles and the metal-support interaction can boost hydrogen generation. A step-by-step reduction method was used to prepare $Pt_{0.25\%}Co_{3\%}/TiO_2$; the TOF was up to 2250 min^{-1} during AB hydrolysis. The introduction of CoO species leads to the formation of electron defects in the interface region of Pt species, which significantly promotes the chemical adsorption and dissociation of water molecules, and accelerates the hydrolysis of AB.[9] Highly dispersed Ru-Cu alloy nanoparticles loaded on nitrogen-doped carbon-coated TiO_2 were successfully prepared by the organic pyrolysis of solid surfaces. The synthesized catalyst exhibits a TOF of 626 min^{-1}; the ensemble-boosting effect significantly promotes the hydrogen generation.[115] Atomic layer deposition strategy was used to treat the Pt-Ni interface and a TOF of 751.6 min^{-1} was obtained. The high activity is attributed to the construction of a specific interface structure.[116] The α-MoC supported Co/Ni catalysts were synthesized using the impregnation method. The TOF was reached 321.1 min^{-1}; the strong metal support interaction (SMSI) effect is responsible for the improvement in activity.[15] From the above-mentioned research, the other methods also have a positive impact on hydrogen generation. Although different strategies have different effects on structure construction, the common emphasis is the rational design of catalysts based on different active structures to enhance catalytic activity. Research on other methods to obtain catalysts may be a direction for future review writing to present the types of catalysts derived from those methods.

CATALYTIC MECHANISM: A UNIVERSAL VOEW FOR BORON HYDROLYSIS

The process of heterogeneous catalytic reaction is the combination of a series of physical and chemical processes. The determination and understanding of catalytic mechanism have always been a key and difficult point in the field of heterogeneous catalysis. For the hydrolysis reaction of boron hydride, the possible forms or pathways of Co substances exist in the hydrolysis reaction. During the hydrolysis reaction, the valence state of Co may exist in the zero or another valence state and then become an acid site; Co also exists in the form of a redox site. For example, zero-valent Co exists as a coordination center. Zero-valent and divalent Co can form an ionic redox cycle and serve as a redox

site. For the hydrogen generation of boron hydride, there are four types of possible mechanisms depending on the microstructure and properties of catalysts. Although the mechanism is suitable for heterogeneous catalysis, it is also appropriate for Co-based catalysts. Illustratively, Co as an active substance has an induction period during the hydrogen generation of boron hydride. The surface reconstruction of Co will occur, and it is still necessary to investigate in depth what happened to the Co substance. Due to the lack of detailed and profound experimental characterization, the understanding of surface reconstruction is not deep enough, and maybe Operando technology can provide help to monitor the mechanism in the future. Currently, the catalytic mechanism of hydrogen generation of AB hydrolysis presents a dissociation mechanism based on oxidative addition-reduction elimination, pre-activation mechanism, SN2 mechanism, four-membered ring mechanism, and acid-base mechanism. In this review, the five catalytic mechanisms are analyzed in detail.

Dissociation mechanism based on oxidative addition-reduction elimination

Oxidative addition and reductive elimination mechanism as a fundamental processes was observed and have always been a concern of transition metal chemistry in various heterogeneous fields, such as the redox-neutral electrochemical conversion of CO_2,[117] photosensitization, and C−H carbometallation.[118] Based on this, a plausible catalytic mechanism for the oxidation addition of O−H and reductive elimination of hydrogen during AB hydrolysis is investigated. Namely, $[H_3NBH_2H]\cdots H{-}OH$ hydrogen bonding resulting from the hydridic property of the B−H bond is suggested here to play a key role. A hydridic B−H is proposed to transfer the H atom to the surface of NPs, this is called the oxidative addition of the B−H bond on the surface. The hydridic surface has the beneficial to close the acidic H atom in H_2O through electrostatic interaction. The dissociation of O–H bond in H_2O and B–H bond in AB forms the intermediates of M−H bonds on the surface of catalyst through oxidative addition. Then, the generation of hydrogen releases from the surface of the catalysts through reductive elimination. This hypothesis provides further theoretical direction for the catalytic mechanism of AB hydrolysis.

Illustratively, the oxidative addition of the O−H bond in H_2O was the rate-determining step (RDS) during the reaction. The effect of favorable OH^- for monometallic or bimetallic NPs of the electronic structure of the NPs on the oxidative addition of H_2O[119] (Figure 7A). AuNi@ZIF-8 alloys are synthesized through $NaBH_4$ reduction and convey excellent performance for hydrogen generation upon AB hydrolysis and the catalytic mechanism was also dissected. The first hydridic surface ligand formed upon hydride transfer from AB and the second hydridic ligand formed upon H_2O activation, eventually after "walking" near each other on the surface via successive bridging (μ2) hydride bonds reductively eliminate to form hydrogen. The cleavage of O–H bonds from H_2O is the RDS, B–H bonds from AB forming the intermediates M–H bonds and further reductive elimination is boosted by visible light irradiation to release hydrogen[28] (Figure 7B). Ni_2Pt@ZIF-8 was prepared through simple one-step $NaBH_4$ reduction and express excellent hydrogen generation from AB hydrolysis. During the mechanism of catalytic reaction, the H_2O molecule forms a hydrogen bond $[NH_3BH_2H]\cdots H{-}OH$ because of the hydridic character of B−H bond. The oxidative addition of the O−H bond of H_2O occurs in the RDS and is validated by the results of the large KIE obtained with D_2O[120] (Figure 7C).

Additionally, during the hydrogen generation of AB, the dissociation mechanism based on oxidative addition-reduction elimination refers to the dissociation of the B−H bond in the AB molecule and O−H bond in the H_2O molecule on the surfaces of catalysts with the generation of H racial and then the hydrogen molecule release from the catalyst surfaces. Based on this, much research has been done on the catalytic dissociative mechanism of metal-based catalysts, such as Co, Ni, Fe-based catalysts,[14,121–124] Co-based phosphide catalyst,[2,102] noble metal-based catalysts and the metal hybrids.[3,39,115,125] In this research, the dissociative mechanism was discussed in detail. Firstly, AB, H_2O, and catalysts are independent states. Subsequently, AB and H_2O molecules are adsorbed on the surface of the catalysts through the constructed dual-active sites, respectively. Then, NH_3BH_3* and H_2O* are formed. H_2O* will dissociate into OH* and H*. The B−H bond in NH_3BH_3* breaks to form NH_3BH_2* and H*. Then, the generated H radical derived from the O−H bond in H_2O* and B−H bond in NH_3BH_3* generates a hydrogen molecule released from the surface of active catalyst. Simultaneously, NH_3BH_2* will attack OH* to NH_3BH_2* and generate of NH_3BH_2OH*. Then, based on this, the other H radical will form in the following dissociation pathway until the other two H_2 molecules are generated according to a similar reaction pathway. Illustratively, in this research, the construction of the dual-active sites is central for the hydrogen generation. The dual-active sites are responsible for the absorption and dissociation of AB and H_2O molecules. The rational design of the catalysts with high-efficiency active sites can enhance the hydrogen generation of catalysts. In real heterogeneous catalysis, several steps are carried out at the same time via some multipoint interaction. The synchronous adsorption/dissociation of AB and H_2O and the interaction in the complex intermediate contribute to the overall catalytic reaction and lead to easier kinetics for the catalytic reaction. The directive dissociative mechanism will provide theoretical guidance and an easy understanding of the catalytic mechanism. Generally, under the in-depth understanding of active structure in catalysts, the design of dual-active sites provides theoretical validation for the catalytic activities toward hydrogen generation. In detail, the design of Ru-Fe nanoalloys supported on N-doped carbon as efficient catalysts has an excellent promotion for hydrogen generation from AB[35] (Figure 8A). Additionally, atomically dispersed Pt on the surface of Ni particles enhanced the hydrogen generation of AB.[126] The simulation results indicate that the high activity achieved stems from the synergistic effect between Pt and Ni, where the negatively charged Pt ($Pt^{\delta-}$) and positively charged Ni ($Ni^{\delta+}$) in the Pt−Ni alloy are prone to interact with H and OH of H_2O molecules, respectively, leading to an energetically favorable reaction pathway (Figure 8B). Noteworthily, in the process of the direct dissociation mechanism, the resultant NH_3BH_2 from the dissociative adsorption of AB on the surface of the catalyst promotes dissociation of H_2O* followed by the B–H bond cleavage of $NH_3BH_2(OH)$*. The reaction of NH_3BH_2*+H_2O* → $NH_3BH_2(OH)$*+H* is irreversible and this is the most likely RDS.[127] Some discussions are performed to study the non-metal doping in the improvement of the catalytic activity. A unique atomic-bridge structure in B-Co-P (namely Co-B and Co-P) dual-active sites on boron nitride nanosheets to stimulate activity toward borohydride hydrolysis was described. Both experimental investigation and theoretical calculations reveal the key effects of atomic-bridge structure in B-Co-P interfacial dual-active sites on tailoring the electron density of Co species and reducing the energy barrier of reaction

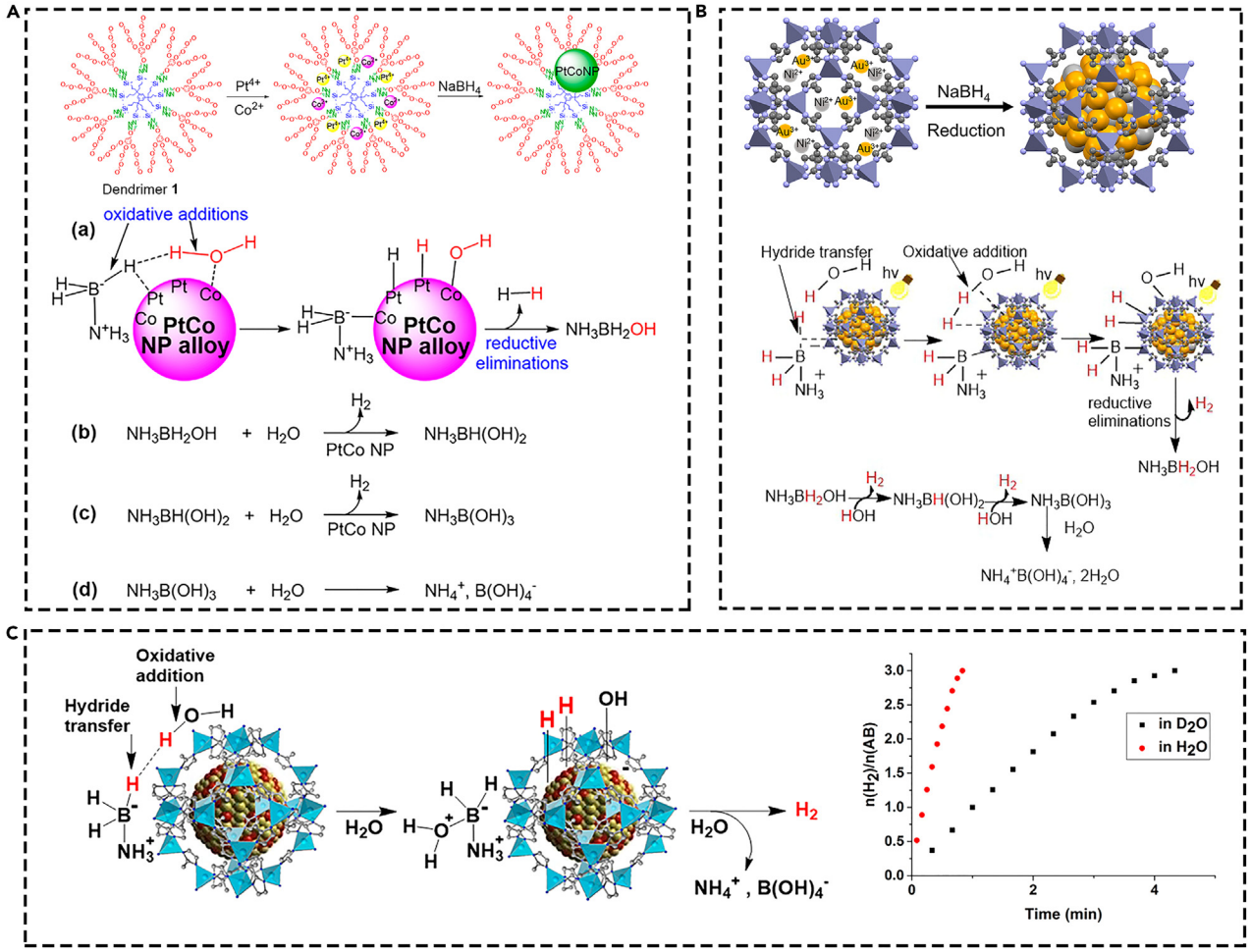

Figure 7. The oxidative addition and reductive elimination mechanism for hydrogen generation catalyzed by

(A) Pt1Co1/1. Reproduced with permission,[119] Copyright 2019, American Chemical Society.

(B) AuNi@ZIF-8. Reproduced with permission,[28] Copyright 2023, Elsevier.

(C) NiPt@ZIF-8 NPs. Reproduced with permission,[120] Copyright 2018, American Chemical Society.

between AB and water molecules[2] (Figure 8C). Polar O-Co-P surface containing Co-O and Co-P active sites for enhancing the bimolecular activation in catalytic hydrogen generation of AB and the corresponding DFT calculations were operated[102] (Figure 8D). The integration of morphology and electronic structure modulation on cobalt phosphide nanosheets to boost photocatalytic hydrogen generation from AB hydrolysis are discussed[128] (Figure 8E). The introduction of the P element into catalysts adjusts the electronic structure and constructs the novel active sites, thus making attribution to the hydrogen generation. Through the experimental results and DFT calculation, the above-mentioned construction of the active sites significantly fabricates the hydrogen generation. Additionally, NiCoP/TiO_2 sensitized system was used to construct a highly unbalanced charge distribution for rapid hydrogen generation under visible light and presented a rate from 0.18 mL s^{-1} in darkness and 0.36 mL s^{-1} under visible light. The optimization of the band structure ensures electron injection from NiCoP to TiO_2. Under visible light, NiCoP is excited and injects electrons into TiO_2, generating a highly unbalanced but stable charge distribution. The positively and negatively charged NiCoP and TiO_2 serve as activation sites for AB and H_2O, respectively.[129] Summarily, Ni-Co-P is the sensitizer and TiO_2 is the electron acceptor, which is expected to construct a stable and unbalanced surface to boost the hydrolytic hydrogen generation by photo-irradiation. The O–H bond in H_2O is cleavage after attacking the adsorbed AB and the two H radicals generated from the O–H bond and B–H bond. Subsequently, a hydrogen molecular was released from the surface of the catalyst.

The above-related mechanism is parallel to the mechanism of oxidative addition-reduction elimination. The difference is that the reaction molecules begin to react under the status of incomplete dissociation in the mechanism of oxidation addition and reductive elimination. Although oxidative addition-reduction elimination mechanism is more in accordance with actual circumstances, some challenges still exist in the investigation because of the complexity of the catalytic reaction. The related dissociation mechanism grasps the main contradiction in the catalytic reaction and facilitates the analysis of hydrogen generation for AB hydrolysis. However, challenges such as the sluggish

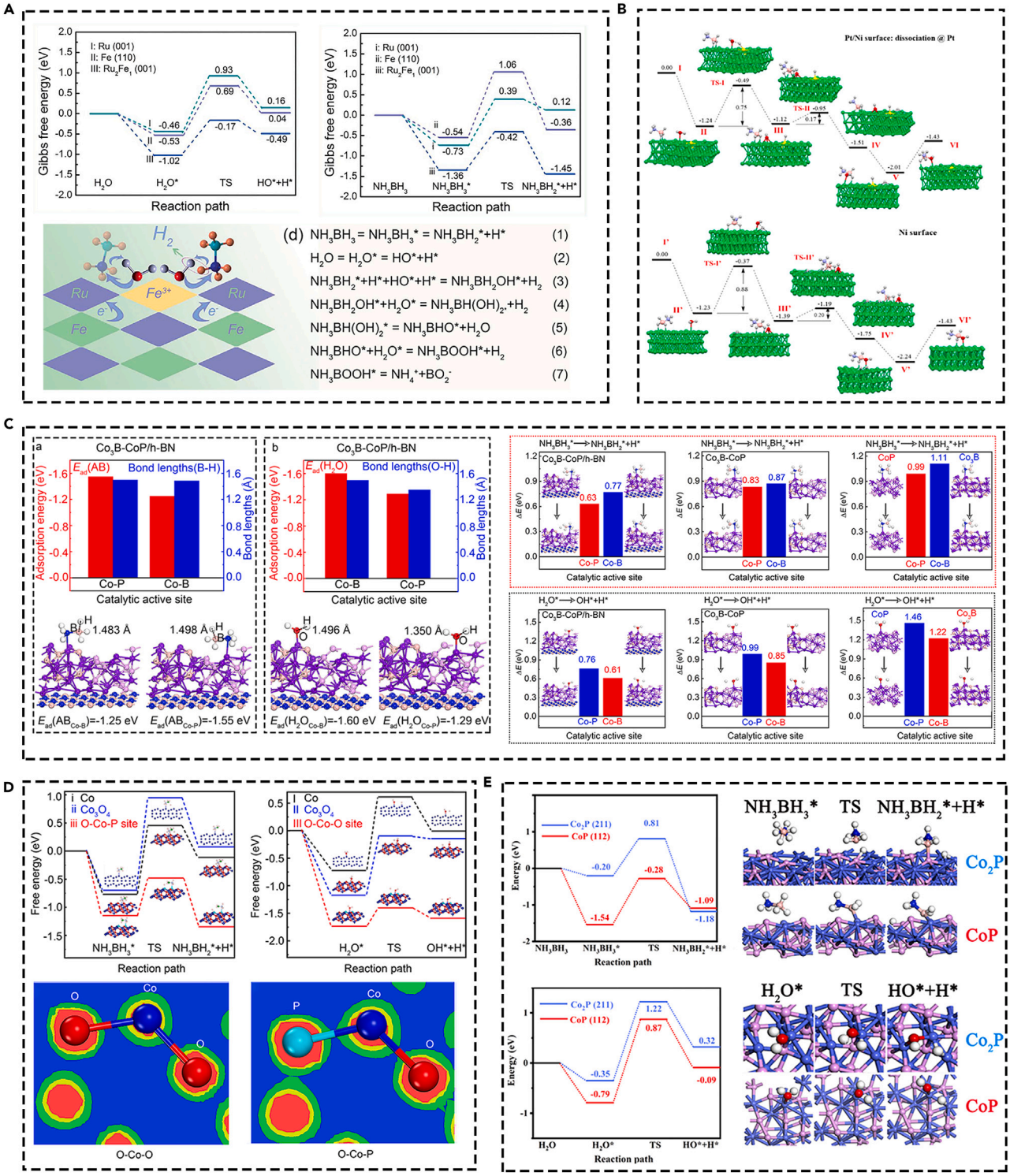

Figure 8. The investigation on the catalytic mechanism of direct dissociation mechanism on surfaces of various catalysts

(A) RuFe/N–C. Reproduced with permission,[35] Copyright 2020, Royal Society of Chemistry.

(B) Pt+Ni/CNT. Reproduced with permission,[126] Copyright 2017, American Chemical Society.

(C) B-Co-P atomic structure. Reproduced with permission,[2] Copyright 2022, Elsevier.

(D) polar Co-P-O surface. Reproduced with permission,[102] Copyright 2022, Elsevier.

(E) CoP-based catalysts. Reproduced with permission,[128] Copyright 2022, KeAi Publishing Ltd.

catalytic kinetics and the unclear catalytic mechanism still exist in the catalytic reaction. Therefore, some endeavors should be applied to investigate the catalytic mechanism.

Pre-activation mechanism

Based on the discussion of the dissociation mechanism involving oxidation addition and reductive elimination, the pre-activation mechanism can be discussed. Generally, the difficulty of the dissociation of the reaction molecules is the key to revealing the role of the active site in the enhancement of the catalytic activity. Illustratively, pre-activation refers to the actions that are auxiliary to the dissociation reaction, which is an auxiliary or preliminary operation. It is paramount for the development of heterogeneous catalysis. The dissociation mechanism based on oxidation addition and reduction elimination is concerned that reaction molecules have a catalytic action with catalysts and then react together independently. In the above-mentioned catalytic mechanism, a pre-activation occurred before the oxidation addition of the H_2O molecule. The H atom in the B−H bond in AB will combine with the H atom in the O−H bond in H_2O and the pre-activation occurs. Subsequently, the hydrogen generation will occur following the dissociation mechanism based on the oxidation addition and elimination reduction.

SN2 mechanism

The SN_2 reaction refers to two molecules involved in a nucleophilic substitution reaction that determines the critical step of the reaction. For the hydrolysis of AB, The SN_2 mechanism refers to the surface OH* attacks the adsorbed BH_3 group in AB and results in the break of B−N bond in AB. When the reaction occurs under general conditions, the AB and H_2O are both adsorbing on the surface of the catalysts. The detailed information is as follows,

(1) Induced B–N bond breaking. Following the SN_2 reaction in which surface OH* attacks the BH_3 group, B–N bond breaking is induced ($OH^*+BH_3NH_3^* \rightarrow BH_3OH^*+NH_3^*$).
(2) B–H bond-breaking. After the B–N bond scission, one of the hydrides leaves the B atom on the surfaces of the catalyst ($BH_3OH^* \rightarrow BH_2OH^* + H^*$).
(3) B–N regeneration. Following the above B–H bond breaking, the regeneration of the B–N bond occurred with almost barrierless. ($BH_2OH^* + NH_3^* \rightarrow HOBH_2–NH_3^*$). Illustratively, the low B–N bond regeneration barrier caused by the electrostatic interaction between B and N atoms results in the B–N bond formation.
(4) First H_2 molecule generation. The hydride group on the surface of the catalyst attacks the H_2O molecule to generate the first H_2 molecule. This process is slightly more exothermic. The first H_2 molecule generation ($NH_3BH_3+H_2O \rightarrow HOBH_2NH_3+H_2$) is released from the surface of the catalysts.

Similarly, after the above-mentioned first reaction cycle, when the species left on the surface are $HOBH_2–NH_3$, it will repeat the previous steps twice and produce two more H_2 molecules from $BH_2(OH)_2^*$ and $BH(OH)_3^*$. We should note that the SN2 step is the rate-limiting step in AB hydrolytic dehydrogenation, which could rationalize the common phenomenon that the presence of OH− could dramatically improve the catalytic properties and shorten the induction period. Xu et al. proposed an attack of H_2O on an activated complex provoking cleavage of the B−N bond and hydrolysis of NH_3 generating hydrogen. As one of the plausible mechanisms, it is reasonable to consider that there should be interactions between the AB molecule and the metal particle surface to form activated complex species, which is most likely the rate-determining step, to which attack by an H_2O molecule readily leads to concerted dissociation of the B–N bonding and hydrolysis of the resulting BH_3 intermediate to produce the borate ion along with the hydrogen release. Interestingly, in the absence of H_2O, dehydro-coupling between AB molecules to form new B–N bonds occurs, probably via a closely related intermediate, on the metal surface.[130] CoNi/α-MoC catalyst was synthesized and used for the robust hydrogen generation from the hydrolysis of AB. For the AB hydrolysis reaction, the synergistic effect of Co−Ni species effectively activated the B−N bond in AB and α-MoC to activate the water and form OH* groups on the surface of the catalyst. The O−H bond cleavage of H_2O combined with the surface OH* attack on the adsorbed AB molecule via the SN_2 mechanism was proposed to be the rate-limiting step. The role of H_2O in the rate-determining step of this reaction was confirmed by an isotopic experiment by replacing H_2O with D_2O (Figure 9A). Additionally, the absorption and reaction of water on the surface of α-MoC and 1.5Co1.5Ni/αMoC were further investigated (Figure 9B). The stoichiometric hydrogen was immediately generated and detected by the mass spectrometer, which demonstrates the cleavage of the O−H bond of water at room temperature forming hydroxyl species (or possibly a very small amount of O* species) that remain on the surface of the catalysts.[15] Ternary Ni–Co–P nanoparticles as noble-metal-free catalysts were used to boost the hydrolytic dehydrogenation of AB and present the SN2 mechanism. In the analysis of the catalytic mechanism, the promotion of electron transfer from metal to P center in these ternary Ni–Co–P solutions, finally results in strong adsorption of AB, which can effectively activate the B–N bonds in AB, therefore decreasing the reaction energy barrier and accelerating hydrogen evolution.[32] Moreover, the synergistic effect between Ni, Co, and P in the $Ni_{0.66}Co_{0.19}P_{0.15}$ NPs and the synergistic electronic effect between NiCoP nanoparticles and the OPC-300, further leading to strong adsorption of AB, which could efficiently motivate the B–N bonds in AB with an SN2 mechanism, hence decreasing the reaction energy barrier and stimulating hydrogen evolution[36] (Figure 9C).

Four-membered ring mechanism

On the other hand, the formation of ring-mounted intermediate during AB hydrolysis with methanol or water as the solvent is reported, and the key effect of the catalytic mechanism based on ring-mounted intermediate also holds promise on providing the theoretical guidance for the hydrogen generation of AB hydrolysis.[129,131] A plausible mechanism for AB methanolysis catalyzed by Rh/PC-COF is proposed (Figure 10).

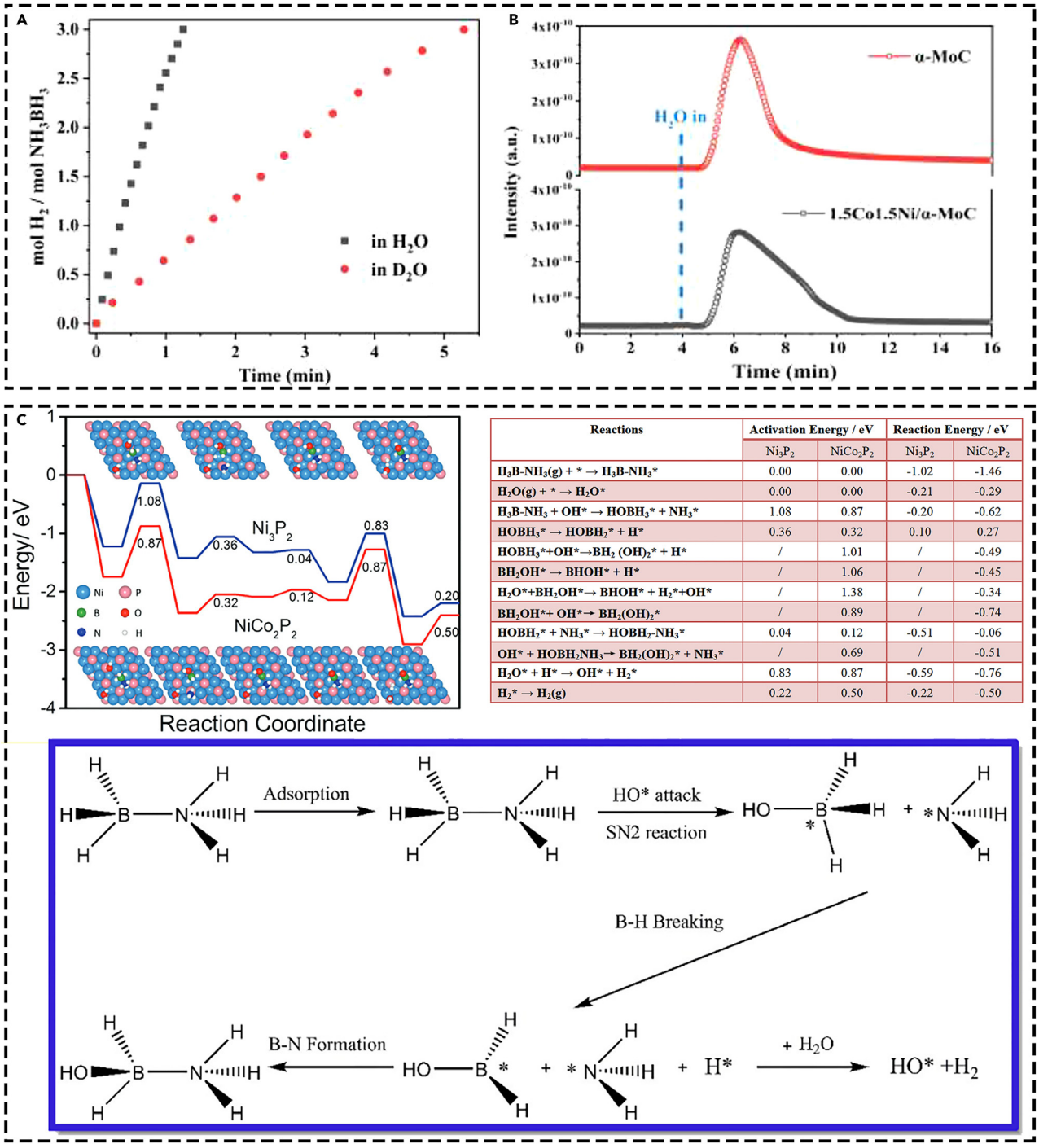

Reactions	Activation Energy / eV		Reaction Energy / eV	
	Ni_3P_2	$NiCo_2P_2$	Ni_3P_2	$NiCo_2P_2$
$H_3B\text{-}NH_3(g) + * \rightarrow H_3B\text{-}NH_3*$	0.00	0.00	-1.02	-1.46
$H_2O(g) + * \rightarrow H_2O*$	0.00	0.00	-0.21	-0.29
$H_3B\text{-}NH_3 + OH* \rightarrow HOBH_3* + NH_3*$	1.08	0.87	-0.20	-0.62
$HOBH_3* \rightarrow HOBH_2* + H*$	0.36	0.32	0.10	0.27
$HOBH_3*+OH* \rightarrow BH_2(OH)_2* + H*$	/	1.01	/	-0.49
$BH_2OH* \rightarrow BHOH* + H*$	/	1.06	/	-0.45
$H_2O*+BH_2OH* \rightarrow BHOH* + H_2*+OH*$	/	1.38	/	-0.34
$BH_2OH*+ OH* \rightarrow BH_2(OH)_2*$	/	0.89	/	-0.74
$HOBH_2* + NH_3* \rightarrow HOBH_2\text{-}NH_3*$	0.04	0.12	-0.51	-0.06
$OH* + HOBH_2NH_3* \rightarrow BH_2(OH)_2* + NH_3*$	/	0.69	/	-0.51
$H_2O* + H* \rightarrow OH* + H_2*$	0.83	0.87	-0.59	-0.76
$H_2* \rightarrow H_2(g)$	0.22	0.50	-0.22	-0.50

Figure 9. The catalytic mechanism analysis on various catalysts

(A) Isotopic experiment of catalytic hydrolysis of AB in H_2O and D_2O, and (B) H_2 (m/z = 2, by mass spectroscopy) formation from water reaction during the hydrolysis of AB by 1.5Co1.5Ni/α-MoC. Reproduced with permission,[15] Copyright 2020, American Chemical Society.

(C) $Ni_{0.7}Co_{1.3}P$/GO. Reproduced with permission,[36] Copyright 2017, Royal Society of Chemistry.

Based on the surface structure of the catalysts, a bonding model (I) is built with electron-rich Rh NPs donated by N species of the COFs. At the first step, an activated complex (II) is formed via the interactions between AB and Rh NPs, which can effectively weaken the B—N bonding. In the second step, the attack of CH_3OH on the weakened B-N bond will easily generate an unstable ring-mounted intermediate consisting of

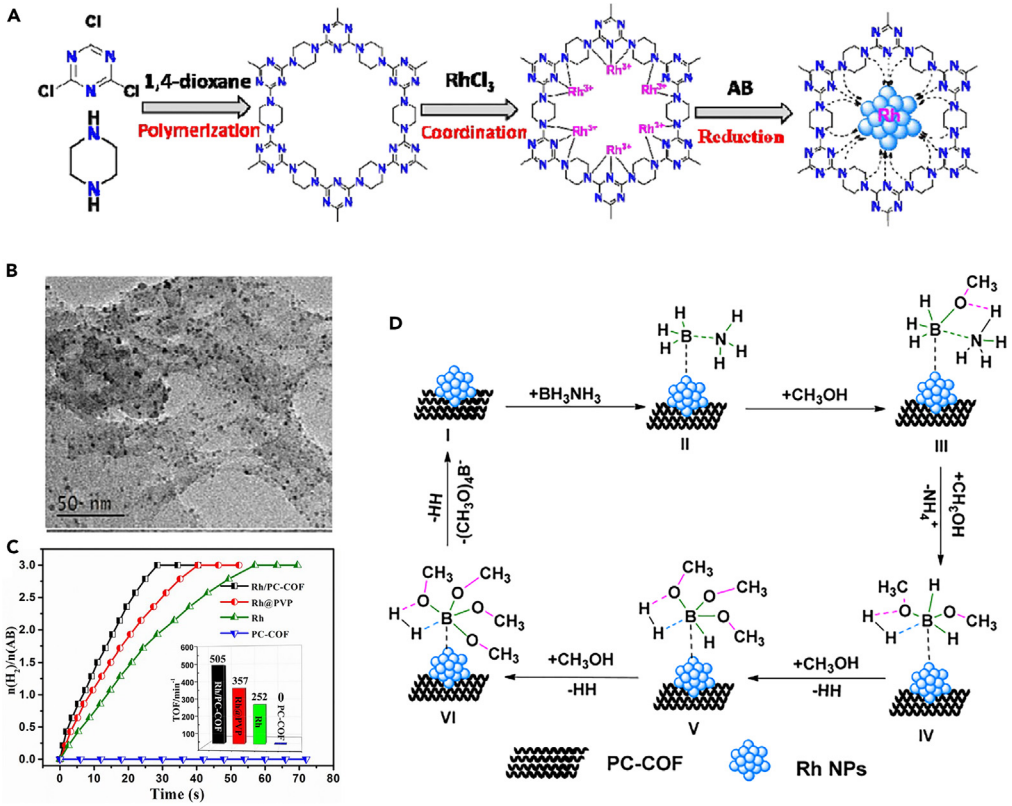

Figure 10. The analysis of four-membered ring mechanism of catalysts on Rh/PC-COF

(A and B) the synthesis and morphologies of Rh/PC-COF.

(C) the catalytic performance of Rh/PC-COF during the hydrolysis of AB.

(D) the proposed mechanism for AB hydrolysis over Rh/PC-COF. Reproduced with permission,[131] Copyright 2020, Royal Society of Chemistry.

B—N···O···H transition state (III). The following attack of another CH_3OH leads to the concerted decomposition of B—N bonding and dissociation of NH_4^+. Meanwhile, another intermediate (IV) containing H—H bonding can be easily formed and released from the surface of the catalysts. The unstable ring-mounted intermediate consists of B-N···O···H transition state (III) and the attack of CH_3OH plays a key role in the hydrogen generation. Collectively, these facts and speculations suggest that the insights into the catalytic mechanism provide effective theoretical guidance in the analysis of the catalytic mechanism catalysis field.[131]

Acid-base mechanism

Acid-base theory refers to the substances that can donate protons are acids (proton acids); and the substances that can accept protons are bases (proton bases). The corresponding proton acids donate the protons and generate the proton bases and the proton bases accept the protons and generate proton acids. Generally, the hydrogen ions in H_2O exist in the format of hydrated protons (H_3O^+). Namely, the H^+ bonds with the electronic pairs in empty 2px orbital and do not change the primary sp^3 hybridization. During the hydrolysis of AB, the acid-base reaction mechanism is that the release of an H proton derived from the H_2O combined with the electron comes from metal and forms an H atom. The existence of hydroxide (OH^-) attracts the B atom in AB and forms a B—O bond with the release of electrons. The H atom in the B—H bond in AB accepts the electron derived from the formation of the B—O bond and forms H^+. Subsequently, the generated H^+ will give the electron to metal and form the H atom. Then the generated two H atoms combine and generate the first H_2 molecule. The H proton and OH^- occurred in this reaction and thus boosted the hydrogen generation. Illustratively, the metal composition of the catalyst plays a paramount role during the process of the acid-base mechanism. Based on this, Rh single-atom supported on VO_2 (Rh1/VO_2) was prepared and used in the hydrogen generation of AB[132] (Figures 11A and 11B). 120 mL of H_2 were generated within 10 min over Rh1/VO_2 at all of these temperatures (Figure 11C). The excellent performance is attributed to the construction of the Rh single-atom and the existence of the support with the generation of metal–support interactions. The reaction mechanism is the acid-base mechanism (Figure 11D). The activation of a proton can be written as follows,

$$H^+ + e^- + * \rightarrow H^*$$

Corresponding to the acid-base mechanism, the hydrogen will be generated and released from the surface of the metal-based catalysts. As H^+ ions need to take electrons from the catalyst to generate H*. Thus, the high chemical potential of electron value is beneficial to the

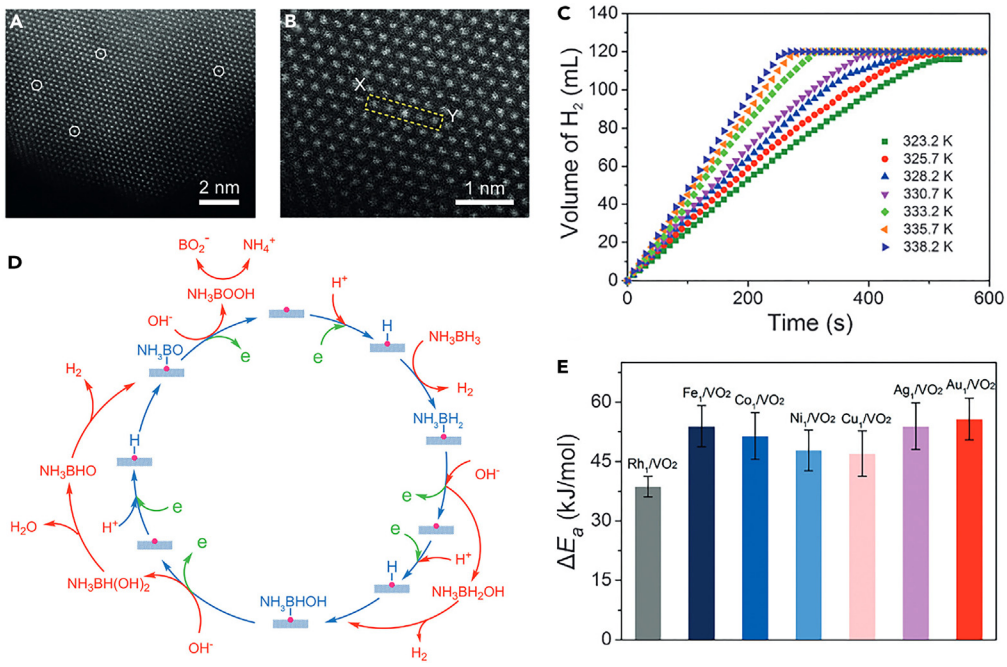

Figure 11. The analysis of acid-base mechanism of catalysts on Rh1/VO_2

(A and B) the morphologies of Rh1/VO_2, (C) the catalytic performance Rh1/VO_2 during the hydrolysis of AB.

(C) Proposed mechanism for AB hydrolysis over Rh1/VO_2.

(D and E) The corresponding mechanism and catalytic activity of catalysts. Reproduced with permission,[132] Copyright 2017, Wiley.

acceleration of the reaction. Thus, in this Rh1/VO_2 catalytic system, some investigation of the reaction was also studied from the perspective of electronic modulation. In the metal–support interaction, the electron transfer from or to support altered the charge state of the metal through the DFT calculations for pure VO_2 and Rh1/VO_2. Furthermore, the mechanistic studies demonstrate that the catalytic performance depended directly on the highest occupied state of the single Rh atoms, which was determined by the band structure of the substrates. Among the different metals, Rh is endowed with the optimal hydrogen adsorption energy and thus has the highest activity among the metals-based catalysts (Figure 11E).

The importance for understanding catalytic processes of various mechanism

The catalytic reaction process usually includes external diffusion, internal diffusion, surface adsorption, surface reaction, surface desorption, internal diffusion, and external diffusion. The occurrence of catalytic reactions mainly depends on the existence of active sites on surfaces. The surface structure of a catalyst has a great influence on its physical, chemical, and electronic structure and other properties. However, it is not easy to study the surface structure of the catalyst clearly because of the surface structure of the catalyst generally changes with the change of its environment and is always in a dynamic equilibrium. Namely, the surface reconstruction including adsorption-induced reconstruction, pretreatment, reconstruction reaction, environmental reconstruction, etc. occurred in the process of the reaction.

From the above-mentioned mechanism, the in-depth understanding of the catalytic process is essential for the unraveling of the catalytic mechanism. Despite these efforts, several mechanistic details remain unresolved and speculative, such as the rate-determining step, the type of the O–H bond cleavage, the order of bond cleavages, as well as the nature of reactant adsorption on metallic surfaces. The confirmation of the rate-determining step (RDS) during the hydrolysis of borohydride is significant for the development of the catalytic reaction. Illustratively, the catalytic mechanisms are different for different catalysts. Thus, how to confirm the rate-determining step is the key scientific challenge in the hydrogen generation process of AB. From the perspective of the hydrogen generation of AB, a plausible pathway was studied in analyzing the RDS. Through the isotopic experiments using D_2O instead of H_2O as a reactant and introducing D_2 into the reaction atmosphere together with other kinetic experiments were carried out to determine the order of B–H, B–N, and O–H bond cleavages and propose a plausible rate-determining step. Therefore, it is significant for us to develop advanced characterization technology, such as the *in situ* and operando to use in the research and characterization of catalytic reaction systems to enable real-time observation (time- and spatially resolved characterization) of structural changes of catalysts and their surface reactions. The application of *in situ* technology to the surface structure characterization of catalysts has become an indispensable and important means to study catalysts and their properties. Fortunately, with the development of *in situ* characterization technology, such as near-normal pressure XPS, near-normal pressure STM, environmental scanning electron microscopy (ESEM), etc. and controllable synthesis technology of materials, such as nanoscale control, morphology control, crystal plane exposure, etc.,

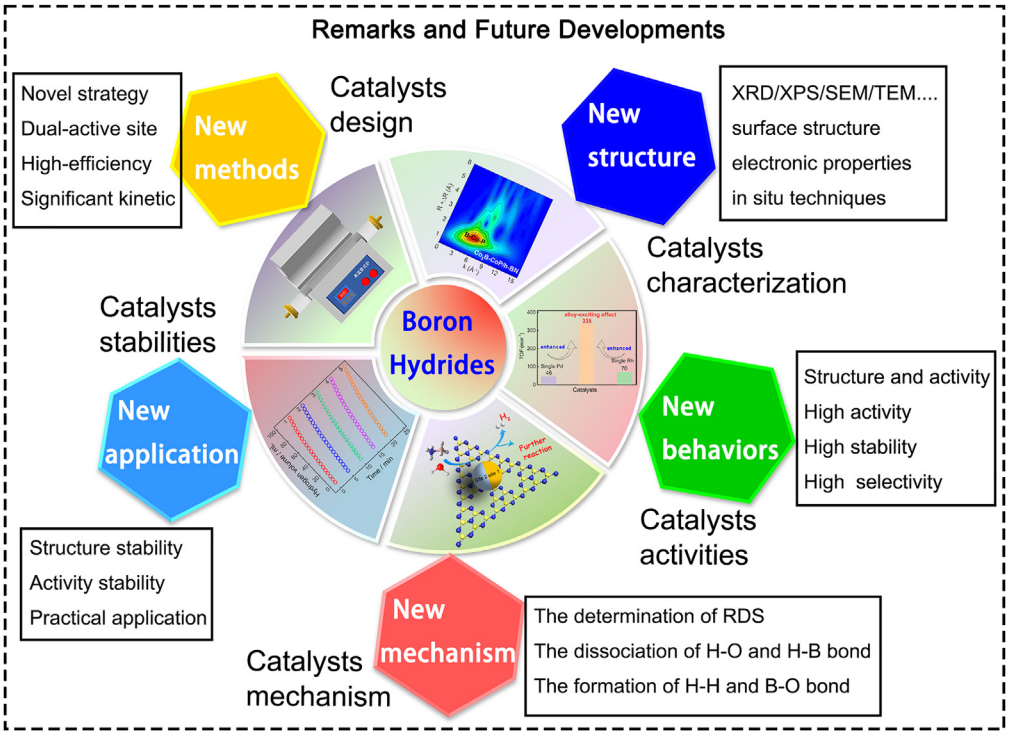

Figure 12. The remarks and further developments of Co-based nanocomposites derived from pyrolysis of organic metal precursor for hydrolysis of boron hydride

the characterization technology is closer to the actual use conditions, and promoting the research on the surface composition and structure of metal oxides, and also promoting the development and progress of catalytic chemistry. In conclusion, the understanding of various mechanism can make contributes to the comprehensive understanding of catalytic processes.

CONCLUSION AND OUTLOOK

In this review, the preparation of Co-based composite materials through pyrolysis and their application in the hydrolysis of boron hydride is investigated in-depth. The corresponding different catalytic mechanisms are also summarized in detail. The different precursors in obtaining Co-based materials through pyrolysis, such as MOF precursor, supported precursor, metal precursor, and MPs precursor were described. Among these different precursors, MOF pyrolysis has been applied most widely because of the feature of easy handling, simplicity, and stable reaction environment. Additionally, with the development of the hydrogen industry, the production process of the traditional preparation of cobalt-based materials has been unable to meet the requirements of further societal development. Thus, abundant efforts are needed to explore suitable methods, such as improving synthetic processes and synthesizing different morphology for controlling particle size to improve the catalytic performance of cobalt-based materials. Additionally, it is important to reveal the catalytic mechanism based on the different structures of catalysts. Although pyrolysis has been extensively studied and can achieve large-scale synthesis, this method still has certain limitations, such as the requirement of high temperature, high energy consumption, large amounts of solvents during preparation, and sample post-processing. These shortcomings severely limit its application in industrial large-scale preparation. Therefore, there is still space and necessary for research in the following aspects by using rational regulation strategy and other regulatory strategies to synergize high-efficiency catalysts and enhance their intrinsic activity. The detailed reflections based on the hydrogen generation of boron hydrides are listed in Figure 12.

The profound exploitation of high-efficiency catalysts

It is vital to rationally explore alternative non-noble metal catalysts. The modification of existing Co-based materials to meet the needs of various applications is worthy of attention and research. Currently, the low activity still is the challenge of Co-based catalysts in the hydrolysis of boron hydride. Although many strategies are taken to synthesize Co-based composite materials, the rational design of highly active and stable catalysts still faces great challenges during the investigation of hydrogen generation for boron hydride. Therefore, the operation of new design strategies and other assistant strategies based on the basic understanding and understanding of catalytic materials on the level of atoms, nanometers, and microscale nanometers are necessary for the enhancement of the catalytic activities of boron hydride. For the

bimolecular reaction of boron hydride, the catalysts should satisfy the dual-active sites. One active site activates H_2O molecule and the other active site activates boron hydride, respectively. Additionally, for the hydrogen generation of boron hydride, the Co-based materials used in industrial applications is promising in the development of hydrogen economy. Thus, the design of monolithic catalysts is vital for the on-demand hydrogen generation in the future. In a nutshell, the preparation of catalysts with high-efficient active sites through adjusting the composition and structure of active ingredients is significant for the hydrogen generation. Through slight changes in the stoichiometric ratio of different substances or reaction conditions can synthesize high-efficiency catalysts. The purpose of catalyst design is embodied in: 1. Conveying significant kinetic changes and generate microstructures with different physicochemical properties; 2. Preventing migration and aggregation in the preparation of catalysts; 3. Combining with advanced design strategies and other auxiliary strategies, such as nano-scale control, morphology control, and crystal plane exposure, to adjust and stabilize the composition and structure of catalysts is necessary for the catalyst design.

The urgent development of advanced characterizations technologies

The characterization of the surface structure and electronic properties of Co-based catalysts is significant for the hydrogen generation of boron hydride. The characterizations of catalysts are important for understanding the coordination structure of the active sites and the interaction between substrate and adsorbate. Therefore, the development of available characterization techniques to present the chemical state of active sites in Co-based catalysts, and understand the control mechanisms of catalytic processes at the atomic level provides a structural foundation. From the perspective of this review, developing new types of catalysts by using non-noble metals to prepare efficient catalysts and break through the catalytic activity of existing precious and non-precious metals is the key to the rapid development of the hydrogen economy. Moreover, the chemical compositions and the phase structures are important for confirming the phase compositions of materials. The research on the different structures of catalysts requires in-depth research at the molecular atomic level in combining *in situ* analysis techniques and computational chemistry in the future. The excavation of novel characterization methods has promising in studying the dynamic influence mechanism and designing the catalysts with high performance in the future.

The dramatical improvement of catalytic activities of catalysts

Catalytic activity is a key descriptor for the rational design of efficient catalysts. Although noble metal-based catalysts exhibit excellent performance in catalytic hydrogen generation, the high price and low reserves hamper the application of noble-based catalysts. Non-noble metal-based catalysts have low catalytic activity and poor stability and have broad development space to meet future applications. For the hydrogen generation of boron hydride based on Co-based catalysts, The catalytic reaction of boron hydride mainly depends on the presence of catalytic active sites. Through the experiments of hydrolysis kinetics, we can to evaluate of catalytic performance and future analyze the real catalytic activity. The design of catalytic active sites with a high exposure ratio and utilization efficiency to improve the catalytic activity of metals is important for enhancing catalytic activity. Therefore, using reasonable design strategies to establish the structure of the catalytic active site, and clarify the catalytic mechanism is significant for improving the catalytic activity and stability. It is necessary to analyze and reveal the catalytic activity and catalytic mechanism through the investigation of catalytic kinetics, *in situ* characterization techniques, and theoretical calculations, which will provide a guidance for the promotion of activity.

The investigation in-depth systematically of catalytic mechanism

Heterogeneous catalytic reactions involve many complex physical and chemical reactions. Understanding the structure-activity relationship of Co-based catalysts is one of the important methods for studying the reaction mechanism and constructing the optimal catalytic system. For Co-based catalysts, revealing of catalytic mechanism is crucial for developing hydrogen generation. Determining the rate determining step, the type of O−H bond dissociation, the order of bond dissociation, and the properties of reactants adsorbing on metal surfaces is critical to understanding the catalytic mechanism of catalysts. However, it is still challenging to clarify the catalytic mechanism for different Co-based active substances or other active ingredients in the process of hydrogen generation for boron hydride. Additionally, the combination of experimental research and theoretical simulation analysis is necessary to clarify the structure-activity relationship in the process of catalytic reaction. During the hydrogen generation of boron hydride, the structure and energy analysis of key steps and conversion mechanisms such as adsorption strength, adsorption mode, the bond breakage of H−O and H−B, and the formation of H−H bond and B−O bond also should be studied. Based on the above-mentioned narration, the combination of advanced technologies such as density functional theory, *in situ* spectroscopies, and conventional tests is promising for the analysis of possible reaction intermediates during the hydrogen generation of boron hydride.

The enhancement of catalytic stability of catalysts

The catalytic stability of active structures is helpful for the investigation of the relationship between structural changes and the stability of catalysts. Through the characterizations of electronic structure and related species valence of the recycled catalysts after reaction, the catalyst structure can be analyzed in detail. Additionally, the correlation between catalytic activity and catalyst structure and valence state of active species provides basic research for improving catalyst activity and improving the cycle stability of catalysts. Moreover, the structure of active sites for the recycled catalysts can be confirmed through spectroscopic characterization. Thus, the real active sites of the catalysts in the catalytic reactions can be identified based on the experimental and theoretical results.

In summary, for the hydrogen generation of boron hydride based on Co-based catalysts. The design of catalysts, the characterization of catalysts, and the catalytic mechanism for the catalytic reaction are important for the development of hydrogen generation. Moreover, it is important to clarify the structures of catalytic active sites and the catalytic mechanism of Co-based catalysts. The structure of the active sites of the catalyst can be clarified through spectroscopic characterization. Combining with the experimental results of boron hydride hydrolysis, the catalytic activity of the catalyst can be evaluated, and the correlation of the active site was also studied. Additionally, the adsorption mode and adsorption activation energy of the reaction species at the active site can be simulated and calculated by DFT. In a nutshell, the correlation between the regulation of the active structure of metal-based catalysts and the catalytic mechanism for hydrogen generation can be studied from both experimental and theoretical levels. From the above-mentioned fundamental narrations, the potential application of the created and optimized metal catalyst in the hydrolysis of boron hydride and other hydrogen storage materials for hydrogen generation and important catalytic reactions related to the activation of water molecules can be further expanded.

ACKNOWLEDGMENTS

Financial supports from the National Natural Science Foundation of China (no. 22279118, no. 22279117, no. 22075254), the National Science Fund for Distinguished Young of China (no. 22225202), the Young Top Talent Program of Zhongyuan-Yingcai-Jihua (no. 30602674), Jiangsu Province Key Laboratory of Biomass Energy and Materials (no. JSBEM-S-201906), and the Top-Notch Talent Program of Henan Agricultural University (no. 30501034) are acknowledged.

AUTHOR CONTRIBUTIONS

H.Z., designed this project, wrote the original draft, provided suggestions, and carefully revised the manuscript. S.L., T.L., R.S., X.G., X.W., Y.L., Y.W., B.L., and E.L. performed formal analysis. Y.L. and B.L., designed this project equally, conducted project administration, and provided suggestions. Y.L., X.G., X.W., Y.W., and B.L. provide funding acquisition. All the authors discussed the results and commented on the manuscript.

DECLARATION OF INTERESTS

The authors declare no competing interests.

REFERENCES

1. Zhan, W.-W., Zhu, Q.-L., and Xu, Q. (2016). Dehydrogenation of ammonia borane by metal nanoparticle catalysts. ACS Catal. *6*, 6892–6905.
2. Zhang, H., Liu, Y., Wei, H., Wang, C., Liu, T., Wu, X., Ashraf, S., Mehdi, S., Guan, S., Fan, Y., et al. (2022). Atomic-bridge structure in B-Co-P dual-active sites on boron nitride nanosheets for catalytic hydrogen generation. Appl. Catal. B Environ. *314*, 121495.
3. Shen, R., Liu, Y., Wen, H., Wu, X., Han, G., Yue, X., Mehdi, S., Liu, T., Cao, H., Liang, E., and Li, B. (2022). Engineering bimodal oxygen vacancies and Pt to boost the activity toward water dissociation. Small *18*, 2105588.
4. Zhang, L., Zhang, K., Wang, C., Liu, Y., Wu, X., Peng, Z., Cao, H., Li, B., and Jiang, J. (2021). Advances and prospects in metal–organic frameworks as key nexus for chemocatalytic hydrogen production. Small *17*, 2102201.
5. Demirci, U.B., and Miele, P. (2014). Cobalt-based catalysts for the hydrolysis of $NaBH_4$ and NH_3BH_3. Phys. Chem. Chem. Phys. *16*, 6872–6885.
6. Shahzad, A., Rafiq, K., Zeeshan Abid, M., Ahmad Khan, N., Shoaib Ahmad Shah, S., Althomali, R.H., Rauf, A., and Hussain, E. (2024). Escalating the synergism on CdZnS via Ag_2S/Cu_2S co-catalysts: boosts hydrogen evolution from water splitting under sunlight. J. Catal. *429*, 115210.
7. Sabir, M., Rafiq, K., Abid, M.Z., Quyyum, U., Shah, S.S.A., Faizan, M., Rauf, A., Iqbal, S., and Hussain, E. (2023). Growth of tunable Au-BaO@TiO_2/CdS heterostructures: acceleration of hydrogen evolution from water splitting. Fuel *353*, 129196.
8. Sahar, K.U., Rafiq, K., Abid, M.Z., Rauf, A., Rehman, U.U., Nadeem, M.A., Jin, R., and Hussain, E. (2023). Sun-light driven hydrogen generation by Pd/Rb_2O cocatalysts: Escalate the utility of rutile TiO_2 for photocatalytic water splitting. Colloids Surf. A Physicochem. Eng. Asp. *674*, 131942.
9. Sahar, K.U., Rafiq, K., Abid, M.Z., Ur Rehman, U., Rauf, A., and Hussain, E. (2023). Surface sensitization of g-C_3N_4/TiO_2 *via* Pd/Rb_2O co-catalysts: accelerating water splitting reaction for green fuel production in the absence of organic sacrificial agents. React. Chem. Eng. *8*, 2522–2536.
10. Saleem, F., Abid, M.Z., Rafiq, K., Rauf, A., Ahmad, K., Iqbal, S., Jin, R., and Hussain, E. (2024). Synergistic effect of Cu/Ni cocatalysts on CdS for sun-light driven hydrogen generation from water splitting. Int. J. Hydrogen Energy *52*, 305–319.
11. Hussain, E., Majeed, I., Nadeem, M.A., Badshah, A., Chen, Y., Nadeem, M.A., and Jin, R. (2016). Titania-supported palladium/strontium nanoparticles (Pd/Sr-NPs@P25) for photocatalytic H_2 production from water splitting. J. Phys. Chem. C *120*, 17205–17213.
12. Wang, L.-C., Chen, B., and Wu, X.-F. (2022). Cobalt-catalyzed direct aminocarbonylation of ethers: efficient access to α-amide substituted ether derivatives. Angew. Chem. Int. Ed. *61*, e202203797.
13. Liu, Y., Han, G., Zhang, X., Xing, C., Du, C., Cao, H., and Li, B. (2017). Co-Co_3O_4@carbon core–shells derived from metal−organic framework nanocrystals as efficient hydrogen evolution catalysts. Nano Res. *10*, 3035–3048.
14. Xu, W., Zhang, S., Shen, R., Peng, Z., Liu, B., Li, J., Zhang, Z., and Li, B. (2023). A catalytic copper/cobalt oxide interface for efficient hydrogen generation. Energy Environ. Mater. *6*, e12279.
15. Ge, Y., Qin, X., Li, A., Deng, Y., Lin, L., Zhang, M., Yu, Q., Li, S., Peng, M., Xu, Y., et al. (2021). Maximizing the synergistic effect of CoNi catalyst on α-MoC for robust hydrogen production. J. Am. Chem. Soc. *143*, 628–633.
16. Jiang, F., Li, Y., and Pan, Y. (2024). Design principles of single-atom catalysts for oxygen evolution reaction: from targeted structures to active sites. Adv. Mater. *36*, 2306309.
17. Fu, X., Shi, R., Jiao, S., Li, M., and Li, Q. (2022). Structural design for electrocatalytic water splitting to realize industrial-scale deployment: Strategies, advances, and perspectives. J. Energy Chem. *70*, 129–153.
18. Hu, L., Wei, X.-Y., and Zong, Z.-M. (2021). Ru/Hβ catalyst prepared by the deposition-precipitation method for enhancing hydrodeoxygenation ability of guaiacol and lignin-derived bio-oil to produce hydrocarbons. J. Energy Inst. *97*, 48–57.
19. Li, H., Chen, L., Jin, P., Li, Y., Pang, J., Hou, J., Peng, S., Wang, G., and Shi, Y. (2022). $NiCo_2S_4$ microspheres grown on N, S co-doped reduced graphene oxide as an efficient bifunctional electrocatalyst for overall water splitting in alkaline and neutral pH. Nano Res. *15*, 950–958.
20. Yang, Z., Wang, H., Fei, X., Wang, W., Zhao, Y., Wang, X., Tan, X., Zhao, Q., Wang, H., Zhu, J., et al. (2021). MOF derived bimetallic

CuBi catalysts with ultra-wide potential window for high-efficient electrochemical reduction of CO_2 to formate. Appl. Catal. B Environ. *298*, 120571.
21. Cui, L., Fan, K., Zong, L., Lu, F., Zhou, M., Li, B., Zhang, L., Feng, L., Li, X., Chen, Y., and Wang, L. (2022). Sol-gel pore-sealing strategy imparts tailored electronic structure to the atomically dispersed Ru sites for efficient oxygen reduction reaction. Energy Storage Mater. *44*, 469–476.
22. Li, H., Berbille, A., Zhao, X., Wang, Z., Tang, W., and Wang, Z.L. (2023). A contact-electro-catalytic cathode recycling method for spent lithium-ion batteries. Nat. Energy *8*, 1137–1144.
23. Liu, B., Lv, N., Wang, C., Zhang, H., Yue, Y., Xu, J., Bi, X., and Bao, X. (2022). Redistributing Cu species in Cu-SSZ-13 zeolite as NH_3-SCR catalyst via a simple ion-exchange. Chin. J. Chem. Eng. *41*, 329–341.
24. Liu, D., Li, J., Ding, S., Lyu, Z., Feng, S., Tian, H., Huyan, C., Xu, M., Li, T., Du, D., et al. (2020). 2D single-atom catalyst with optimized iron sites produced by thermal melting of metal–organic frameworks for oxygen reduction reaction. Small Methods *4*, 1900827.
25. Guan, S., Liu, Y., Zhang, H., Shen, R., Wen, H., Kang, N., Zhou, J., Liu, B., Fan, Y., Jiang, J., and Li, B. (2023). Recent advances and perspectives on supported catalysts for heterogeneous hydrogen production from ammonia borane. Adv. Sci. *10*, 2300726.
26. Zhang, X., Zhang, L., Zhang, W., Ren, Z., Huang, Z., Hu, J., Gao, M., Pan, H., and Liu, Y. (2021). Nano-synergy enables highly reversible storage of 9.2 wt% hydrogen at mild conditions with lithium borohydride. Nano Energy *83*, 105839.
27. Martínez, A.A., Gasnier, A., and Gennari, F.C. (2022). Pore filling of a carbon matrix by melt-impregnated $LiBH_4$. J. Phys. Chem. C *126*, 66–78.
28. Kang, N., Wei, X., Shen, R., Li, B., Cal, E.G., Moya, S., Salmon, L., Wang, C., Coy, E., Berlande, M., et al. (2023). Fast Au-Ni@ZIF-8-catalyzed ammonia borane hydrolysis boosted by dramatic volcano-type synergy and plasmonic acceleration. Appl. Catal. B Environ. *320*, 121957.
29. Zhang, A., Xia, J., Yao, Q., and Lu, Z.-H. (2022). Pd–WO_x heterostructures immobilized by MOFs-derived carbon cage for formic acid dehydrogenation. Appl. Catal. B Environ. *309*, 121278.
30. Zhang, Z., Lu, Z.-H., Tan, H., Chen, X., and Yao, Q. (2015). CeO_x-modified RhNi nanoparticles grown on rGO as highly efficient catalysts for complete hydrogen generation from hydrazine borane and hydrazine. J. Mater. Chem. A *3*, 23520–23529.
31. Zhang, Z., Zhang, S., Yao, Q., Feng, G., Zhu, M., and Lu, Z.-H. (2018). Metal–organic framework immobilized RhNi alloy nanoparticles for complete H_2 evolution from hydrazine borane and hydrous hydrazine. Inorg. Chem. Front. *5*, 370–377.
32. Hou, C.-C., Li, Q., Wang, C.-J., Peng, C.-Y., Chen, Q.-Q., Ye, H.-F., Fu, W.-F., Che, C.-M., López, N., and Chen, Y. (2017). Ternary Ni–Co–P nanoparticles as noble-metal-free catalysts to boost the hydrolytic dehydrogenation of ammonia-borane. Energy Environ. Sci. *10*, 1770–1776.
33. Guo, L.-T., Cai, Y.-Y., Ge, J.-M., Zhang, Y.-N., Gong, L.-H., Li, X.-H., Wang, K.-X., Ren, Q.-Z., Su, J., and Chen, J.-S. (2015). Multifunctional Au–Co@CN nanocatalyst for highly efficient hydrolysis of ammonia borane. ACS Catal. *5*, 388–392.
34. Liao, J., Shao, Y., Feng, Y., Zhang, J., Song, C., Zeng, W., Tang, J., Dong, H., Liu, Q., and Li, H. (2023). Interfacial charge transfer induced dual-active-sites of heterostructured $Cu_{0.8}Ni_{0.2}WO_4$ nanoparticles in ammonia borane methanolysis for fast hydrogen production. Appl. Catal. B Environ. *320*, 121973.
35. Zhou, D., Huang, X., Wen, H., Shen, R., Liu, Y., Guo, X., and Li, B. (2020). Ru–Fe nanoalloys supported on N-doped carbon as efficient catalysts for hydrogen generation from ammonia borane. Sustain. Energy Fuels *4*, 3677–3686.
36. Qu, X., Jiang, R., Li, Q., Zeng, F., Zheng, X., Xu, Z., Chen, C., and Peng, J. (2019). The hydrolysis of ammonia borane catalyzed by NiCoP/OPC-300 nanocatalysts: high selectivity and efficiency, and mechanism. Green Chem. *21*, 850–860.
37. Cai, J., Ding, J., Wei, D., Xie, X., Li, B., Lu, S., Zhang, J., Liu, Y., Cai, Q., and Zang, S. (2021). Coupling of Ru and O-vacancy on 2D Mo-based electrocatalyst via a solid-phase interface reaction strategy for hydrogen evolution reaction. Adv. Energy Mater. *11*, 2100141.
38. Zhang, H., Fan, Y., Liu, B., Liu, Y., Ashraf, S., Wu, X., Han, G., Gao, J., and Li, B. (2019). Birdcage-type CoO_x-carbon catalyst derived from metal–organic frameworks for enhanced hydrogen generation. ACS Sustain. Chem. Eng. *7*, 9782–9792.
39. Shen, R., Liu, Y., Wen, H., Liu, T., Peng, Z., Wu, X., Ge, X., Mehdi, S., Cao, H., Liang, E., et al. (2022). Engineering V_O-Ti ensemble to boost the activity of Ru towards water dissociation for catalytic hydrogen generation. Appl. Catal. B Environ. *306*, 121100.
40. Zhang, X., Sun, X., Xu, D., Tao, X., Dai, P., Guo, Q., and Liu, X. (2019). Synthesis of MOF-derived Co@C composites and application for efficient hydrolysis of sodium borohydride. Appl. Surf. Sci. *469*, 764–769.
41. Lin, K.-Y.A., and Chang, H.-A. (2016). Efficient hydrogen production from $NaBH_4$ hydrolysis catalyzed by a magnetic cobalt/carbon composite derived from a zeolitic imidazolate framework. Chem. Eng. J. *296*, 243–251.
42. Zhou, L., Meng, J., Li, P., Tao, Z., Mai, L., and Chen, J. (2017). Ultrasmall cobalt nanoparticles supported on nitrogen-doped porous carbon nanowires for hydrogen evolution from ammonia borane. Mater. Horiz. *4*, 268–273.
43. Gao, Z., Ding, C., Wang, J., Ding, G., Xue, Y., Zhang, Y., Zhang, K., Liu, P., and Gao, X. (2019). Cobalt nanoparticles packaged into nitrogen-doped porous carbon derived from metal-organic framework nanocrystals for hydrogen production by hydrolysis of sodium borohydride. Int. J. Hydrogen Energy *44*, 8365–8375.
44. Chen, M., Xiong, R., Cui, X., Wang, Q., and Liu, X. (2019). SiO_2-Encompassed Co@N-doped porous carbon assemblies as recyclable catalysts for efficient hydrolysis of ammonia borane. Langmuir *35*, 671–677.
45. Xing, C., Liu, Y., Su, Y., Chen, Y., Hao, S., Wu, X., Wang, X., Cao, H., and Li, B. (2016). Structural evolution of Co-based metal organic frameworks in pyrolysis for synthesis of core–shells on nanosheets: Co@CoO_x@Carbon-rGO composites for enhanced hydrogen generation activity. ACS Appl. Mater. Interfaces *8*, 15430–15438.
46. Liu, K., Jiang, L., Huang, W., Zhu, G., Zhang, Y.-J., Xu, C., Qin, R., Liu, P., Hu, C., Wang, J., et al. (2022). Atomic overlayer of permeable microporous cuprous oxide on palladium promotes hydrogenation catalysis. Nat. Commun. *13*, 2597.
47. Xu, K., Ma, C., Yan, H., Gu, H., Wang, W.-W., Li, S.-Q., Meng, Q.-L., Shao, W.-P., Ding, G.-H., Wang, F.R., and Jia, C.J. (2022). Catalytically efficient Ni-NiO_x-Y_2O_3 interface for medium temperature water-gas shift reaction. Nat. Commun. *13*, 2443.
48. Wang, H., Wang, L., Lin, D., Feng, X., Niu, Y., Zhang, B., and Xiao, F.-S. (2021). Strong metal–support interactions on gold nanoparticle catalysts achieved through Le Chatelier's principle. Nat. Catal. *4*, 418–424.
49. Li, R., Liu, Z., Trinh, Q.T., Miao, Z., Chen, S., Qian, K., Wong, R.J., Xi, S., Yan, Y., Borgna, A., et al. (2021). Strong metal–support interaction for 2D materials: application in noble Metal/TiB_2 heterointerfaces and their enhanced catalytic performance for formic acid dehydrogenation. Adv. Mater. *33*, 2101536.
50. Wang, W., Zhai, W., Chen, Y., He, Q., and Zhang, H. (2022). Two-dimensional material-based virus detection. Sci. China Chem. *65*, 497–513.
51. Duan, S., Han, G., Su, Y., Zhang, X., Liu, Y., Wu, X., and Li, B. (2016). Magnetic Co@g-C_3N_4 core–shells on rGO sheets for momentum transfer with catalytic activity toward continuous-flow hydrogen generation. Langmuir *32*, 6272–6281.
52. Wu, X., Zhang, X., Han, G., Liu, Y., Liu, B., Gao, J., Fan, Y., and Li, B. (2018). Reaction of Co_3O_4 nanocrystals on graphene sheets to fabricate excellent catalysts for hydrogen generation. ACS Sustain. Chem. Eng. *6*, 8427–8436.
53. Wang, L., Liu, Y., Ashraf, S., Jiang, J., Han, G., Gao, J., Wu, X., and Li, B. (2019). Pitaya pulp structural cobalt–carbon composite for efficient hydrogen generation from borohydride hydrolysis. J. Alloys Compd. *808*, 151774.
54. Zhang, X., Wei, Z., Guo, Q., and Tian, H. (2013). Kinetics of sodium borohydride hydrolysis catalyzed via carbon nanosheets supported Zr/Co. J. Power Sources *231*, 190–196.
55. Zhu, J., Li, R., Niu, W., Wu, Y., and Gou, X. (2012). Facile hydrogen generation using colloidal carbon supported cobalt to catalyze hydrolysis of sodium borohydride. J. Power Sources *211*, 33–39.
56. Zou, Y., Yin, Y., Gao, Y., Xiang, C., Chu, H., Qiu, S., Yan, E., Xu, F., and Sun, L. (2018). Chitosan-mediated Co–Ce–B nanoparticles for catalyzing the hydrolysis of sodium borohydride. Int. J. Hydrogen Energy *43*, 4912–4921.
57. Wang, H., Zhao, Y., Cheng, F., Tao, Z., and Chen, J. (2016). Cobalt nanoparticles embedded in porous N-doped carbon as long-life catalysts for hydrolysis of ammonia borane. Catal. Sci. Technol. *6*, 3443–3448.
58. Mahmood, J., Jung, S.-M., Kim, S.-J., Park, J., Yoo, J.-W., and Baek, J.-B. (2015). Cobalt oxide encapsulated in C_2N-*h* 2D network polymer as a catalyst for hydrogen evolution. Chem. Mater. *27*, 4860–4864.
59. Huang, Y., Wang, Y., Zhao, R., Shen, P.K., and Wei, Z. (2008). Accurately measuring the hydrogen generation rate for hydrolysis of sodium borohydride on multiwalled carbon

nanotubes/Co–B catalysts. Int. J. Hydrogen Energy *33*, 7110–7115.
60. Xu, D., Lu, P., Dai, P., Wang, H., and Ji, S. (2012). In situ synthesis of multiwalled carbon nanotubes over $LaNiO_3$ as support of cobalt nanoclusters catalyst for catalytic applications. J. Phys. Chem. C *116*, 3405–3413.
61. Zhang, F., Ma, C., Zhang, Y., Li, H., Fu, D., Du, X., and Zhang, X.-M. (2018). N-doped mesoporous carbon embedded Co nanoparticles for highly efficient and stable H_2 generation from hydrolysis of ammonia borane. J. Power Sources *399*, 89–97.
62. Fan, D., Lv, X., Feng, J., Zhang, S., Bai, J., Lu, R., and Liu, J. (2017). Cobalt nickel nanoparticles encapsulated within hexagonal boron nitride as stable, catalytic dehydrogenation nanoreactor. Int. J. Hydrogen Energy *42*, 11312–11320.
63. Wang, N., Sun, Q., Zhang, T., Mayoral, A., Li, L., Zhou, X., Xu, J., Zhang, P., and Yu, J. (2021). Impregnating subnanometer metallic nanocatalysts into self-pillared zeolite nanosheets. J. Am. Chem. Soc. *143*, 6905–6914.
64. Shu, H., Lu, L., Zhu, S., Liu, M., Zhu, Y., Ni, J., Ruan, Z., and Liu, Y. (2019). Ultra small cobalt nanoparticles supported on MCM41: One-pot synthesis and catalytic hydrogen production from alkaline borohydride. Catal. Commun. *118*, 30–34.
65. Luo, Y.-C., Liu, Y.-H., Hung, Y., Liu, X.-Y., and Mou, C.-Y. (2013). Mesoporous silica supported cobalt catalysts for hydrogen generation in hydrolysis of ammonia borane. Int. J. Hydrogen Energy *38*, 7280–7290.
66. Murathan, H.B., Özkan, G., Akkuş, M.S., Özgür, D.Ö., and Özkan, G. (2018). Hydrogen production from the methanolysis of ammonia borane by Pd-Co/Al_2O_3 coated monolithic catalyst. Int. J. Hydrogen Energy *43*, 10728–10733.
67. Liu, Q., Zhang, S., Liao, J., Huang, X., Zheng, Y., and Li, H. (2017). $MnCo_2O_4$ film composed of nanoplates: synthesis, characterization and its superior catalytic performance in the hydrolytic dehydrogenation of ammonia borane. Catal. Sci. Technol. *7*, 3573–3579.
68. Yuan, Z., Liu, L., Ru, W., Zhou, D., Kuang, Y., Feng, J., Liu, B., and Sun, X. (2022). 3D printed hierarchical spinel monolithic catalysts for highly efficient semi-hydrogenation of acetylene. Nano Res. *15*, 6010–6018.
69. Li, Y., Ma, W., Wang, J., and Zhong, Q. (2022). A NiFe-based monolithic electrocatalyst for pleiotropic-efficiency water oxidation. J. Mater. Chem. A *10*, 24388–24397.
70. Zhang, P., Liu, Y., Wang, S., Zhou, L., Liu, T., Sun, K., Cao, H., Jiang, J., Wu, X., and Li, B. (2022). Wood-derived monolithic catalysts with the ability of activating water molecules for oxygen electrocatalysis. Small *18*, 2202725.
71. Zheng, Y., Su, Y., Pang, C., Yang, L., Song, C., Ji, N., Ma, D., Lu, X., Han, R., and Liu, Q. (2022). Interface-enhanced oxygen vacancies of $CoCuO_x$ catalysts in situ grown on monolithic Cu foam for VOC catalytic oxidation. Environ. Sci. Technol. *56*, 1905–1916.
72. Xie, L., Wang, K., Du, G., Asiri, A.M., and Sun, X. (2017). Self-standing cobalt oxide nanosheet array: an monolithic catalyst for effective hydrolysis of $NaBH_4$ in alkaline media. Int. J. Hydrogen Energy *42*, 30639–30645.
73. Xie, L., Wang, K., Du, G., Asiri, A.M., and Sun, X. (2016). 3D hierarchical CuO/Co_3O_4 core–shell nanowire array on copper foam for on-demand hydrogen generation from alkaline $NaBH_4$ solution. RSC Adv. *6*, 88846–88850.
74. Cui, L., Sun, X., Xu, Y., Yang, W., and Liu, J. (2016). Cobalt carbonate hydroxide nanowire array on Ti mesh: an efficient and robust 3D catalyst for on-demand hydrogen generation from alkaline $NaBH_4$ solution. Chem. Eur J. *22*, 14831–14835.
75. Huang, Y., Wang, K., Cui, L., Zhu, W., Asiri, A.M., and Sun, X. (2016). Effective hydrolysis of sodium borohydride driven by self-supported cobalt oxide nanorod array for on-demand hydrogen generation. Catal. Commun. *87*, 94–97.
76. Dai, H., Liang, Y., Wang, P., Yao, X., Rufford, T., Lu, M., and Cheng, H. (2008). High-performance cobalt–tungsten–boron catalyst supported on Ni foam for hydrogen generation from alkaline sodium borohydride solution. Int. J. Hydrogen Energy *33*, 4405–4412.
77. Wang, H., Li, X., Lan, X., and Wang, T. (2018). Supported ultrafine NiCo bimetallic alloy nanoparticles derived from bimetal–organic frameworks: a highly active catalyst for furfuryl alcohol hydrogenation. ACS Catal. *8*, 2121–2128.
78. Muravev, V., Parastaev, A., van den Bosch, Y., Ligt, B., Claes, N., Bals, S., Kosinov, N., and Hensen, E.J.M. (2023). Size of cerium dioxide support nanocrystals dictates reactivity of highly dispersed palladium catalysts. Science *380*, 1174–1179.
79. Zhou, J., Gao, Z., Xiang, G., Zhai, T., Liu, Z., Zhao, W., Liang, X., and Wang, L. (2022). Interfacial compatibility critically controls Ru/TiO_2 metal-support interaction modes in CO_2 hydrogenation. Nat. Commun. *13*, 327.
80. Tomboc, G.R.M., Tamboli, A.H., and Kim, H. (2017). Synthesis of Co_3O_4 macrocubes catalyst using novel chitosan/urea template for hydrogen generation from sodium borohydride. Energy *121*, 238–245.
81. Durano, M.M., Tamboli, A.H., and Kim, H. (2017). Cobalt oxide synthesized using urea precipitation method as catalyst for the hydrolysis of sodium borohydride. Colloids Surf. A Physicochem. Eng. Asp. *520*, 355–360.
82. Kantürk Figen, A., and Coşkuner, B. (2013). A novel perspective for hydrogen generation from ammonia borane (NH_3BH_3) with Co–B catalysts: "Ultrasonic Hydrolysis. Int. J. Hydrogen Energy *38*, 2824–2835.
83. Li, X., Huang, Y., Chen, Z., Hu, S., Zhu, J., Tsiakaras, P., and Kang Shen, P. (2023). Novel PtNi nanoflowers regulated by a third element (Rh, Ru, Pd) as efficient multifunctional electrocatalysts for ORR, MOR and HER. Chem. Eng. J. *454*, 140131.
84. Zhang, H., Ling, T., and Du, X.-W. (2015). Gas-phase cation exchange toward porous single-crystal CoO nanorods for catalytic hydrogen production. Chem. Mater. *27*, 352–357.
85. Wu, C., Bai, Y., Liu, D.-X., Wu, F., Pang, M.-L., and Yi, B.-L. (2011). Ni–Co–B catalyst-promoted hydrogen generation by hydrolyzing $NaBH_4$ solution for in situ hydrogen supply of portable fuel cells. Catal. Today *170*, 33–39.
86. Zhao, B., Liu, J., Zhou, L., Long, D., Feng, K., Sun, X., and Zhong, J. (2016). Probing the electronic structure of M-graphene oxide (M = Ni, Co, NiCo) catalysts for hydrolytic dehydrogenation of ammonia borane. Appl. Surf. Sci. *362*, 79–85.
87. Barakat, N.A. (2013). Effective Co–Mn–O nanofibers for ammonia borane hydrolysis. Mater. Lett. *106*, 229–232.
88. Qian, L., Jia, D., and Miao, Y. (2019). Nanoporous microspheres of Co-Zn-S as catalysts for oxygen evolution by water splitting and hydrogen generation by ammonia borane hydrolysis. J. Electrochem. Soc. *166*, F18–F23.
89. Liao, J., Lu, D., Diao, G., Zhang, X., Zhao, M., and Li, H. (2018). $Co_{0.8}Cu_{0.2}MoO_4$ microspheres composed of nanoplatelets as a robust catalyst for the hydrolysis of ammonia borane. ACS Sustain. Chem. Eng. *6*, 5843–5851.
90. Barakat, N.A. (2013). Catalytic and photo hydrolysis of ammonia borane complex using Pd-doped Co nanofibers. Appl. Catal. Gen. *451*, 21–27.
91. Li, A., Zhang, L., Wang, F., Zhang, L., Li, L., Chen, H., and Wei, Z. (2022). Rational design of porous Ni-Co-Fe ternary metal phosphides nanobricks as bifunctional electrocatalysts for efficient overall water splitting. Appl. Catal. B Environ. *310*, 121353.
92. Kim, T.-S., Song, H.J., Kim, J.-C., Ju, B., and Kim, D.-W. (2018). 3D architectures of Co_xP using silk fibroin scaffolds: an active and stable electrocatalyst for hydrogen generation in acidic and alkaline media. Small *14*, 1801284.
93. Pan, Y., Sun, K., Liu, S., Cao, X., Wu, K., Cheong, W.-C., Chen, Z., Wang, Y., Li, Y., Liu, Y., et al. (2018). Core–shell ZIF-8@ZIF-67-derived CoP nanoparticle-embedded N-doped carbon nanotube hollow polyhedron for efficient overall water splitting. J. Am. Chem. Soc. *140*, 2610–2618.
94. Zhao, X., Li, X., An, L., Iputera, K., Zhu, J., Gao, P., Liu, R.-S., Peng, Z., Yang, J., and Wang, D. (2022). Nitrogen-inserted nickel nanosheets with controlled orbital hybridization and strain fields for boosted hydrogen oxidation in alkaline electrolytes. Energy Environ. Sci. *15*, 1234–1242.
95. Yang, S., Zhu, J.-Y., Chen, X.-N., Huang, M.-J., Cai, S.-H., Han, J.-Y., and Li, J.-S. (2022). Self-supported bimetallic phosphides with artificial heterointerfaces for enhanced electrochemical water splitting. Appl. Catal. B Environ. *304*, 120914.
96. Liu, J., Liu, X., Shi, H., Luo, J., Wang, L., Liang, J., Li, S., Yang, L.-M., Wang, T., Huang, Y., and Li, Q. (2022). Breaking the scaling relations of oxygen evolution reaction on amorphous NiFeP nanostructures with enhanced activity for overall seawater splitting. Appl. Catal. B Environ. *302*, 120862.
97. Liu, H., Guan, J., Yang, S., Yu, Y., Shao, R., Zhang, Z., Dou, M., Wang, F., and Xu, Q. (2020). Metal–organic-framework-derived Co_2P nanoparticle/multi-doped porous carbon as a trifunctional electrocatalyst. Adv. Mater. *32*, 2003649.
98. Yuan, G., Liu, D., Feng, X., Shao, M., Hao, Z., Sun, T., Yu, H., Ge, H., Zuo, X., and Zhang, Y. (2022). In situ fabrication of porous Co_xP hierarchical nanostructures on carbon fiber cloth with exceptional performance for sodium storage. Adv. Mater. *34*, 2108985.
99. Wang, L., Fan, J., Liu, Y., Chen, M., Lin, Y., Bi, H., Liu, B., Shi, N., Xu, D., Bao, J., and Han,

M. (2021). Phase-modulation of iron/nickel phosphides nanocrystals "Armored" with porous P-doped carbon and anchored on P-doped graphene nanohybrids for enhanced overall water splitting. Adv. Funct. Mater. *31*, 2010912.

100. Quan, Q., Lai, Z., Bao, Y., Bu, X., Meng, Y., Wang, W., Takahashi, T., Hosomi, T., Nagashima, K., Yanagida, T., et al. (2021). Self-anti-stacking 2D metal phosphide loop-sheet heterostructures by edge-topological regulation for highly efficient water oxidation. Small *17*, 2006860.
101. Men, Y., Su, J., Du, X., Liang, L., Cheng, G., and Luo, W. (2018). CoBP nanoparticles supported on three-dimensional nitrogen-doped graphene hydrogel and their superior catalysis for hydrogen generation from hydrolysis of ammonia borane. J. Alloys Compd. *735*, 1271–1276.
102. Zhang, H., Zhang, K., Ashraf, S., Fan, Y., Guan, S., Wu, X., Liu, Y., Liu, B., and Li, B. (2023). Polar O–Co–P surface for bimolecular activation in catalytic hydrogen generation. Energy Environ. Mater. *6*, e12273.
103. Jiang, R., Wang, W., Zheng, X., Li, Q., Xu, Z., and Peng, J. (2021). Hierarchically porous CoP@CNR nanorod derived from metal-organic frameworks as noble-metal-free catalyst for dehydrogenization of ammonia-borane. Int. J. Hydrogen Energy *46*, 5345–5354.
104. Ma, X., He, Y., Zhang, D., Chen, M., Ke, S., Yin, Y., and Chang, G. (2020). Cobalt-based MOF-derived CoP/hierarchical porous carbon (HPC) composites as robust catalyst for efficient dehydrogenation of ammonia-borane. ChemistrySelect *5*, 2190–2196.
105. Hou, C.-C., Chen, Q.-Q., Li, K., Wang, C.-J., Peng, C.-Y., Shi, R., and Chen, Y. (2019). Tailoring three-dimensional porous cobalt phosphides templated from bimetallic metal–organic frameworks as precious metal-free catalysts towards the dehydrogenation of ammonia-borane. J. Mater. Chem. A *7*, 8277–8283.
106. Xiong, C., Zhang, X., Lei, Y., Zhang, L., Shang, H., Zhang, B., and Zhao, Y. (2021). One-pot synthesis of ultrafine $Ni_{0.13}Co_{0.87}P$ nanoparticles on halloysite nanotubes as efficient catalyst for hydrogen evolution from ammonia borane. Appl. Clay Sci. *214*, 106293.
107. Chen, Y., Feng, K., Yuan, G., Kang, Z., and Zhong, J. (2022). Highly efficient CoNiP nanoboxes on graphene oxide for the hydrolysis of ammonia borane. Chem. Eng. J. *428*, 131219.
108. Zhou, X., Meng, X.-F., Wang, J.-M., Shang, N.-Z., Feng, T., Gao, Z.-Y., Zhang, H.-X., Ding, X.-L., Gao, S.-T., Feng, C., and Wang, C. (2019). Boron nitride supported NiCoP nanoparticles as noble metal-free catalyst for highly efficient hydrogen generation from ammonia borane. Int. J. Hydrogen Energy *44*, 4764–4770.
109. Wang, C., Wang, Z., Wang, H., Chi, Y., Wang, M., Cheng, D., Zhang, J., Wu, C., and Zhao, Z. (2021). Noble-metal-free $Co@Co_2P$/N-doped carbon nanotube polyhedron as an efficient catalyst for hydrogen generation from ammonia borane. Int. J. Hydrogen Energy *46*, 9030–9039.
110. Asim, M., Zhang, S., Wang, Y., Maryam, B., Sajid, M., Shi, C., Pan, L., Zhang, X., and Zou, J.-J. (2022). Self-supporting NiCoP for hydrogen generation via hydrolysis of ammonia borane. Fuel *318*, 123544.
111. Yang, L., Wang, K., Du, G., Zhu, W., Cui, L., Zhang, C., Sun, X., and Asiri, A.M. (2016). Cobalt phosphide nanowall arrays supported on carbon cloth: an efficient monolithic non-noble-metal hydrogen evolution catalyst. Nanotechnology *27*, 475702.
112. Liu, T., Wang, K., Du, G., Asiri, A.M., and Sun, X. (2016). Self-supported CoP nanosheet arrays: a non-precious metal catalyst for efficient hydrogen generation from alkaline $NaBH_4$ solution. J. Mater. Chem. A *4*, 13053–13057.
113. Qu, B., Tao, Y., Yang, L., and Liu, Y. (2021). One-pot co-reduction synthesis of orange-like Pd@Co@P nanoparticles supported on rGO for catalytic hydrolysis of ammonia borane. Int. J. Hydrogen Energy *46*, 31324–31333.
114. Wu, H., Zheng, J.n., Zuo, Y.h., Xu, L.x., Ye, M.f., and Wan, C. (2023). Preparation of rice husk-based carbon supported ruthenium catalyst for the hydrolysis of ammonia borane to produce hydrogen. J. Fuel Chem. Technol. *51*, 1201–1208.
115. Huang, X., Liu, Y., Wen, H., Shen, R., Mehdi, S., Wu, X., Liang, E., Guo, X., and Li, B. (2021). Ensemble-boosting effect of Ru-Cu alloy on catalytic activity towards hydrogen evolution in ammonia borane hydrolysis. Appl. Catal. B Environ. *287*, 119960.
116. Zhang, J., Zheng, X., Yu, W., Feng, X., and Qin, Y. (2022). Unravelling the synergy in platinum-nickel bimetal catalysts designed by atomic layer deposition for efficient hydrolytic dehydrogenation of ammonia borane. Appl. Catal. B Environ. *306*, 121116.
117. Lee, K.M., Jang, J.H., Balamurugan, M., Kim, J.E., Jo, Y.I., and Nam, K.T. (2021). Redox-neutral electrochemical conversion of CO_2 to dimethyl carbonate. Nat. Energy *6*, 733–741.
118. Kim, J., Kim, D., and Chang, S. (2020). Merging two functions in a single Rh catalyst system: bimodular conjugate for light-induced oxidative coupling. J. Am. Chem. Soc. *142*, 19052–19057.
119. Wang, Q., Fu, F., Yang, S., Martinez Moro, M., Ramirez, M.d.l.A., Moya, S., Salmon, L., Ruiz, J., and Astruc, D. (2019). Dramatic synergy in CoPt nanocatalysts stabilized by "Click" dendrimers for evolution of hydrogen from hydrolysis of ammonia borane. ACS Catal. *9*, 1110–1119.
120. Fu, F., Wang, C., Wang, Q., Martinez-Villacorta, A.M., Escobar, A., Chong, H., Wang, X., Moya, S., Salmon, L., Fouquet, E., et al. (2018). Highly selective and sharp Volcano-type synergistic Ni_2Pt@ZIF-8-catalyzed hydrogen evolution from ammonia borane hydrolysis. J. Am. Chem. Soc. *140*, 10034–10042.
121. Guan, S., Liu, Y., Zhang, H., Wei, H., Liu, T., Wu, X., Wen, H., Shen, R., Mehdi, S., Ge, X., et al. (2022). Atomic interface-exciting catalysis on cobalt nitride-oxide for accelerating hydrogen generation. Small *18*, 2107417.
122. Guan, S., Zhang, L., Zhang, H., Guo, Y., Liu, B., Wen, H., Fan, Y., and Li, B. (2020). Defect-rich $Co-CoO_x$-graphene nanocatalysts for efficient hydrogen production from ammonia borane. Chem. Asian J. *15*, 3087–3095.
123. Mo, B., Li, S., Wen, H., Zhang, H., Zhang, H., Wu, J., Li, B., and Hou, H. (2022). Functional group regulated $Ni/Ti_3C_2T_x$ (T_x=F, −OH) holding bimolecular activation tunnel for enhanced ammonia borane hydrolysis. ACS Appl. Mater. Interfaces *14*, 16320–16329.
124. Cui, C., Liu, Y., Mehdi, S., Wen, H., Zhou, B., Li, J., and Li, B. (2020). Enhancing effect of Fe-doping on the activity of nano Ni catalyst towards hydrogen evolution from NH_3BH_3. Appl. Catal. B Environ. *265*, 118612.
125. Liu, Y., Wen, H., Zhou, D., Huang, X., Wu, X., Jiang, J., Guo, X., and Li, B. (2021). Tuning surface d charge of Ni-Ru alloys for unprecedented catalytic activity towards hydrogen generation from ammonia borane hydrolysis. Appl. Catal. B Environ. *291*, 120094.
126. Li, Z., He, T., Matsumura, D., Miao, S., Wu, A., Liu, L., Wu, G., and Chen, P. (2017). Atomically dispersed Pt on the surface of Ni particles: synthesis and catalytic function in hydrogen generation from aqueous ammonia–borane. ACS Catal. *7*, 6762–6769.
127. Chen, W., Li, D., Wang, Z., Qian, G., Sui, Z., Duan, X., Zhou, X., Yeboah, I., and Chen, D. (2017). Reaction mechanism and kinetics for hydrolytic dehydrogenation of ammonia borane on a Pt/CNT catalyst. AIChE J. *63*, 60–65.
128. Wan, C., Liang, Y., Zhou, L., Huang, J., Wang, J., Chen, F., Zhan, X., and Cheng, D.g. (2024). Integration of morphology and electronic structure modulation on cobalt phosphide nanosheets to boost photocatalytic hydrogen evolution from ammonia borane hydrolysis. Green Energy Environ. *9*, 333–343.
129. Wang, Y., Shen, G., Zhang, Y., Pan, L., Zhang, X., and Zou, J.-J. (2020). Visible-light-induced unbalanced charge on $NiCoP/TiO_2$ sensitized system for rapid H_2 generation from hydrolysis of ammonia borane. Appl. Catal. B Environ. *260*, 118183.
130. Xu, Q., and Chandra, M. (2006). Catalytic activities of non-noble metals for hydrogen generation from aqueous ammonia–borane at room temperature. J. Power Sources *163*, 364–370.
131. Li, X., Zhang, C., Luo, M., Yao, Q., and Lu, Z.-H. (2020). Ultrafine Rh nanoparticles confined by nitrogen-rich covalent organic frameworks for methanolysis of ammonia borane. Inorg. Chem. Front. *7*, 1298–1306.
132. Wang, L., Li, H., Zhang, W., Zhao, X., Qiu, J., Li, A., Zheng, X., Hu, Z., Si, R., and Zeng, J. (2017). Supported rhodium catalysts for ammonia–borane hydrolysis: dependence of the catalytic activity on the highest occupied state of the single rhodium atoms. Angew. Chem. Int. Ed. *56*, 4712–4718.